ÉCOLE POLYTECHNIQUE
FÉDÉRALE DE LAUSANNE

MACQUARIE
University

Master Thesis – July 2018

Monthly to decadal evolution of sandy beaches in the Pittwater estuary

Figure 1: View of Scotland Island and the Pittwater Estuary
©www.visitsydneyaustralia.com

Author
Vincent De Staercke

Macquarie University Supervisor
Prof. Shari Gallop
EPFL Supervisor
Prof. François Golay

July 27, 2018

Abstract

Even if the total length of shorelines in low-wave environments like bays, sounds, lagoons and estuaries greatly exceed that of open-ocean coasts, the morphodynamics of such systems are poorly understood. Only few studies developed models to predict changes in these environments and these systems are often managed with the same policies as open ocean beaches. The Pittwater estuary is located in the north of Sydney, it is a drowned valley estuary with a well developed flood-tidal delta. The present study investigates the morphodynamics of four beaches in the northern part of this estuary, at two different timescales.

The long term stability of these beaches have been examined using historical aerial photographs that allow to determine the position of the shoreline for the last decades. At the monthly to seasonal timescale, the morphological changes have been studied from beach surveys that are perform every one or two months since May 2016. Given that the survey campaign began just before a major storm that occurred in June 2016, this data set allow to study the post-storm recovery of these sandy estuarine beaches.

The results of the present study show that the beaches within the Pittwater estuary are evolving differently according to parameters like distance from the inlet, exposure to ocean generated waves or beach shape. Examination of the aerial photographs suggest that two out of the four studied beaches are experiencing changes visible over several decades. Concerning the monthly to seasonal changes, detailed analysis of beach surveys indicated that sandy estuarine beaches can be strongly eroded during a storm event and that post-storm recovery can take several years up to decades. The comparison with two beaches located along the open coast in the Sydney area conclude that estuarine beaches have a much slower recovery rate.

Acknowledgements

In the first place, I would like to thank my supervisors : Prof. Shari Gallop, for your availability, help and suggestions throughout the last months and Prof. François Golay, for the support you gave me with this project in Australia. Without you, this adventure at the other end of the world would not have been possible.

I would also like to express special thanks to Thomas Fellowes that introduced me to beach surveying with "Fancy Nancy" and Prof. Ana Vila-Concejo that instructed me about coastal environments and field works methodology. Also to the students from the the Geocoastal Research Group that I met during these fun days of field works in Botany Bay. It was a pleasure to swim, dive, freeze and wait by your side.

To all the friends that I met during these months in Sydney, in particular to the "North Era Crew" that show me the Australian surfer lifestyle and made my stay particularly enjoyable. As well to the explorers who accompanied me during weekends in the Blues Mountains or Nowra. I hope to see you again soon somewhere in the world.

Last but not least, to my parents, Marinette and Thierry, and my brother, Lionel, who always supported me since the beginning of my studies, I owe you so much !

Contents

1 Introduction

From exposed ocean beaches, through estuaries, lakes and reservoirs, coastlines occur in a variety of environments. However, since the late 1960s, research on sandy beaches has focused mainly on open-coast beaches with high wave activity (Eliot et al., 2006). Although, the length of shorelines in lower wave energy environments such as bays, sounds, lagoons and estuaries greatly exceed that of open-ocean coasts (Nordstrom, 1992).

Estuaries are unique ecosystems with exceptional ecological, recreational, and commercial value. They are also some of the most populated regions of the world and rank among the most heavily impacted aquatic ecosystems on earth (Kennish, 2016). However, these complex systems have been given poor attention resulting in a limited knowledge of their morphodynamics and are often managed with the same policies as open ocean beaches (Nordstrom, 1992). This is an issue for sustainable management of estuarine beaches, especially in the perspective of changing storm regimes and sea level rise associated with climate change (Qin et al., 2007).

Nevertheless, recent studies are trying to develop models to predict changes in environments with low wave energy (Eliot et al., 2006, Hegge et al., 1996, Jackson et al., 2002, Nordstrom, 1992, Travers, 2007) but there is still lots of uncertainties about the evolution of these systems.

2 Background

2.1 Estuarine systems

The most widely-used definition for an estuary is the one given by Pritchard (1967) as "a semi-enclosed coastal body of water, which has a free connection with the open sea, and within which sea water is measurably diluted with fresh water derived from land drainage". However, as highlighted by Elliott and McLusky (2002), this definition does not take into account the importance of tides. Thus the definition of Fairbridge (1980) is more suitable. According to him, an estuary is defined as "an inlet of the sea reaching into a river valley as far as the upper limit of tidal rise, usually being divisible into three sectors: (a) a marine or lower estuary, in free connection with the open sea; (b) a middle estuary subject to strong salt and freshwater mixing; and (c) an upper or fluvial estuary, characterized by freshwater but subject to strong tidal action. The limits between these sectors are variable and subject to constant changes in the river discharges".

A classification of estuaries along the eastern Australian coast was made by Roy et al. (2001). He classified estuaries into five groups according to the nature of their entrances that dictates the water exchange between the estuary and sea. The first group consists of *semi-enclosed bays* filled with marine water, such as Botany Bay in Sydney. Then, with large entrance and similar tidal range than the ocean are the *tide-dominated estuaries*. *Wave-dominated estuaries* have lower tidal ranges and are more strongly influenced by river. They are generally found along the coast, behind sand barriers. The group of *intermittent estuaries* comprises the water bodies that are isolated from the sea for extended period of time, it consists of saline or evaporative lagoons for example. The last group is composed of *freshwater bodies* that have from time to time linkage to the sea.

Drowned valley estuaries are included in the *tide-dominated estuaries* group. They occupy deeply incised bedrock valley. On high-energy coastline such as the New South Wales coastline, their mouth usually contains a large marine flood-tidal delta composed of sand derived from the open coast that grows continuously while accommodation space is available in the center part.

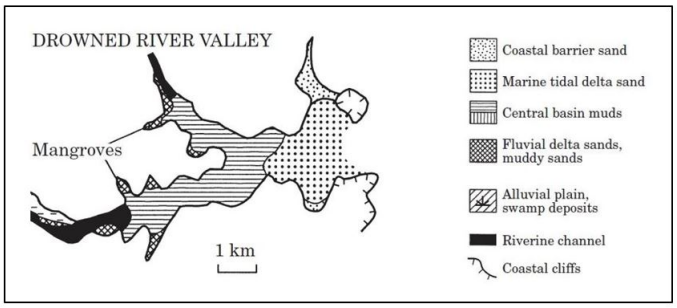

Figure 2: Idealized sediment distribution in tide-dominated estuary, from Roy et al. (2001)

A natural gradient of energy exposure is present across estuary with high-energy and low-energy environments existing side by side. The most energetic section is situated to the seaward-most part of the entrance yet the degree of exposure to open-ocean waves also depend of the orientation of the beaches. The less energetic segment is present in the inner side of the estuaries.

2.2 Beach morphology

Sheltered shorelines in bays, sounds, lagoons and estuaries are called "low-energy" shorelines, derived from the comparison with the "high-energy" open coast beaches. These beaches are characterized by low wave heights, short wave periods and restricted sediment budgets that directly affect the types of topography present in these environments (Nordstrom and Jackson, 2012).

According to Jackson et al. (2002), the term "low-energy" describe an environment that is "fetch-limited", "sheltered" or a combination of both. "Fetch-limited" beaches are controlled by locally generated wind waves that depend on the wind speed, direction and duration as well as characteristics of the basin. "Sheltered" environments are mostly affected by swell wave that are attenuated by island, submerged barriers or other offshore structures. These two types of beaches are not exclusive and usually, low-energy environment is affected by both local and non-local waves. This is the case for most estuarine environments ; estuarine beaches that are located near the ocean inlet are mostly affected by ocean-generated waves while the better sheltered ones will especially experience locally generated wind waves. Jackson et al. (2002) proposed four criteria to define what a low-energy beach is : (1) non-storm significant wave heights are minimal (<0.25 m); (2) significant wave heights due to strong onshore winds are low (<0.50 m); (3) beach face widths are narrow (<20 m in microtidal environments) and (4) morphologic features include those inherited from higher energy events.

According to Jackson (1995), estuarine beaches are generally characterized by a narrow or absent backshore, a steep foreshore and a large low-tide terrace. At the back of the beach, dunes can develop depending on the supply of sediments and the winds. With these characteristics, estuarine beaches can be classified as reflective sandy beaches (Short, 2007). Small wave height is required for a beach to be reflective (<0.5 m) and this type of beach is generally found in harbors, estuaries and at the extremity of some ocean beaches. Because of the small wave height and the relatively deep nearshore zone (> 1 m), the waves break at the beach face and the energy must be dissipated over a very short distance. The main part of the energy goes to the wave swash but a part of this energy is reflected back to the sea, hence the name.

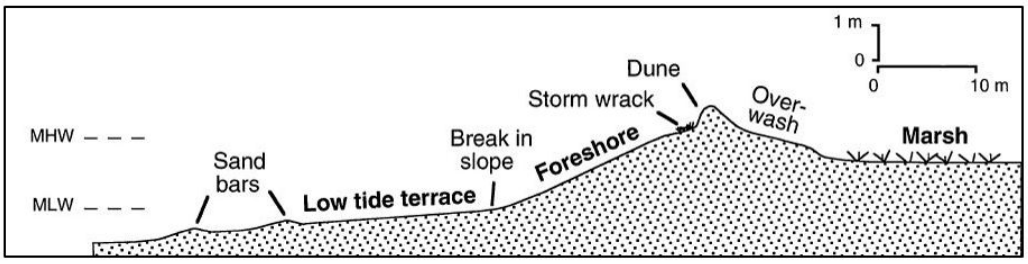

Figure 3: Typical profile for estuarine beaches , modified from Jackson (1995)

2.3 Beach profile dynamics

The majority of the research about dynamics of beach have been conducted in high-energy wave-dominated environments where surf zone processes and rip currents are the driving factors for morphologic changes. In low-energy environments, beach morphodynamics have been investigated by authors such as Hegge et al. (1996), Jackson (1995), Makaske and Augustinus (1998), Nordstrom (1992).

The beach face, defined as the area on the beach were swash and back-swash are active, is a highly dynamic environment and quickly respond to change in water levels or wave conditions (Makaske and Augustinus, 1998). Nordstrom (1992) proposed two types of profile response to changing wave energy on sheltered sandy beaches that will depend on the dominant sediment transport mode (rather cross- or longshore). The first type is caused by transfer of sediment from the upper to the lower foreshore resulting in a concave profile. Erosion of the upper foreshore is caused by an increase in the wave height whereas when the wave energy decrease, sediment is brought back to the upper foreshore. The second is linked to longshore current activity that can be caused by changes in wind direction or wave angle causing a parallel retreat of the foreshore.

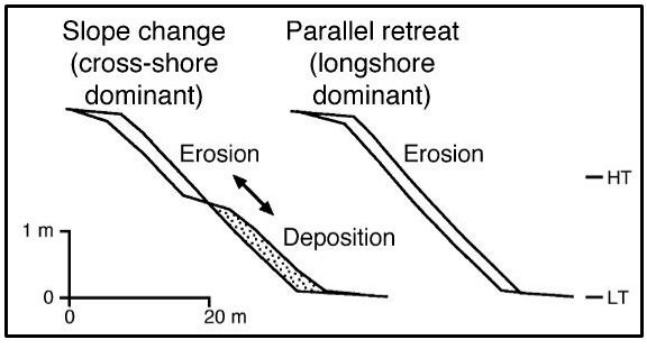

Figure 4: Profile changes for low-energy beaches from Nordstrom (1992).

This lack of diversity in beach shapes has been questioned by Hegge et al. (1996) who developed a four morphotypes profile classification : (1) concave ; (2) moderately concave ; (3) moderately steep ; (4) stepped. According to the authors, these beach forms are generally associated with different types of sediment since physical processes were similar during the duration of their study.

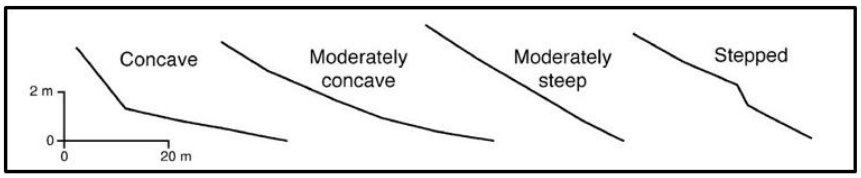

Figure 5: low-energy beach morphotypes from Hegge et al. (1996).

The statement from Hegge et al. (1996) that profile types are more related to sediment characteristics than physical conditions has raised questions in the relation between forms and processes. Authors like Hegge et al. (1996), Jackson et al. (2002), Travers (2007) consider that the morphology of low-energy beaches are mostly affected by short term variations in wave energy caused by storms or strong winds. Thus, observed morphology could be relic from the last high-energy event since modal conditions following these events may not be sufficient to return beach to their original conditions. That is why Hegge et al. (1996) called attention on the fact that further research is needed to assess the impact of storm events and strong sea breeze on low-energy beaches and their recovery.

2.4 Post-storm recovery

Beaches located near the entrance of an estuary can develop conditions of high-energy environments and be strongly impacted by ocean generated waves (Roy et al., 2001). These periods are normally followed by phases of beach recovery. Calm conditions during a long period of time are necessary for the beach to get back to the pre-storm morphology (Harley et al., 2017b). However post-storm beach recovery of low-energy beaches can be slower than for moderate-high-energy sandy beaches because of restricted alongshore sediment supply and insufficient wave energy following a storm (Jackson et al., 2002). According to Houser et al. (2015), there are numerous descriptions of near-instantaneous beach and dune erosion due to storms but only few studies about long term beach and dune recovery. This is especially true for estuarine beaches that have receive poor attention resulting in poor understanding of the post-storm recovery of these systems (Vila-Concejo et al., 2010). Nevertheless, post-storm recovery of low-energy beaches located along microtidal and storm-dominated coastlines have been assessed by several studies (Costas et al., 2005, Jackson, 1995, Maspataud et al., 2009, Morton et al., 1994).

The sandy beaches located along the southeastern coast of Texas, a microtidal area where wave energy is generally low and erosion mainly occurring during storm events, have been studied by Morton et al. (1994). Following a hurricane that happened in 1983, regular beach surveys were done for 10 year. The authors identified four stages of beach recovery. The first one is a rapid accretion of the forebeach with the sand that was stored directly offshore being redeposited by wave runup. This stage lasts between few months and one year. The second stage involves subaerial deposition of sand as consequence of minor flooding of the backbeach and aeolian transport. The two last stages involve dune formation, expansion and recolonization by the vegetation. In this study site, 5 out of the seven profile sites didn't return to their pre-storm conditions even ten years after the storm. According to the authors, the complete recovery of the beach will depend on the sand supply and the long term shoreline displacement.

Costas et al. (2005) studied a sheltered, low-energy beach located in the Iberian Peninsula for three years. The authors noticed that the beach was eroded during high-energy event and that beach recovery was observed during fair weather conditions. However, wave conditions were insufficient to allow a full beach recovery between storms events and therefore beach morphology may indicate a state of partial recovery rather than equilibrium conditions.

Regarding high-energy open coastline or barrier island beaches, several authors have studied the evolution of beach profiles during period of accretion and erosion (Harley et al., 2017b, Loureiro et al., 2012, Thom and Hall, 1991). To mention just a few, Harley et al. (2017b) have been studied the recovery following a major storm event in six representative embayed beaches along the New South Wales coastline. Results showed that these beaches quickly recovered after an high-energy event (51% of subaerial volume recovery six months after a major storm that happened in June 2016). However, this observation does not apply to every high-energy beaches. Loureiro et al. (2012) investigated some embayed beaches located along the high-energy southwestern coast of Portugal and showed that due to the presence of strong rip currents, these beaches were not recovering in the month following a storm. Nevertheless, compared to low-energy environments, the wave energy and the amount of sediment supply in these high-energy systems are generally higher and should favour the post-storm recovery of these environments (Jackson et al., 2002).

In the perspective of changing storm regimes and sea level rise associated with climate change (Qin et al., 2007), understanding the recovery of beaches after a high-energy event is important. Especially when the erosion of a beach generally occurs over a short-period of time while it can take years to decades before the beach and dune are able to return to their pre-storm state (Houser et al., 2015).

2.5 Aim and objectives

The present study aims to give a better understanding of the evolution of sandy estuarine beaches using two data sets at different time scales : short term data that allow to study the monthly to seasonal changes of the profiles and long term data that look at the decadal evolution of shorelines. This study have three main objectives. First, investigate the decadal evolution of shorelines from aerial and satellite images and assess the long term stability of the studied beaches. Second, quantify the short term variability of the different beach profiles that are monthly surveyed with Real Time Kinematic GPS since May 2016. The third objective is to compare the post-storm recovery of sandy estuarine beaches with two embayed beaches located along the open coast in New South Wales.

3 Study Area

The region concerned by this study is the Sydney area within the state of New South Wales (NSW) in Australia. Along the NSW coast, there are more than 900 water bodies that are open to the Pacific Ocean. Most of them are small ephemeral creeks or drains but among them are found 57 estuaries (Roy et al., 2001).

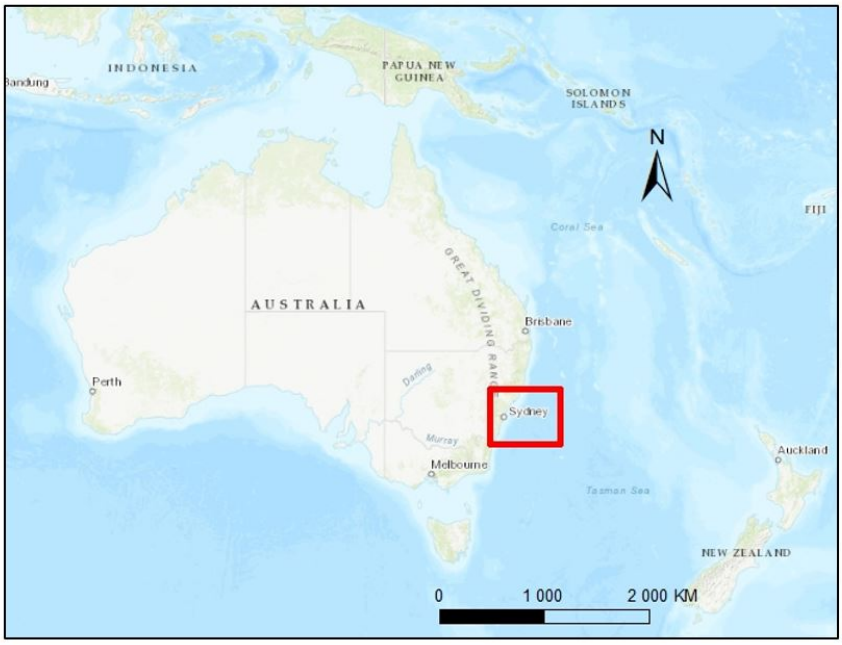

Figure 6: Location of the Sydney area, within the state of New South Wales in Australia. ©ESRI Atla

3.1 The Pittwater estuary and the studied beaches

The Pittwater estuary is located approximately 40 km north of Sydney central business district. As visible on Figure 7, the estuary flows north between West Head and Barrenjoey Head, towards Broken Bay, the confluence of the Hawkesbury River, Pittwater, and Brisbane Water. The mouth of the Pittwater estuary is located less than 1 km west from the Tasman Sea.

It can be observed on Figure 7 that the eastern part of the catchment is largely urbanized with the suburbs of Mona Vale, Avalon and Warriewood while the western part is primarily in the perimeter of the Ku-ring-gai Chase National Park.

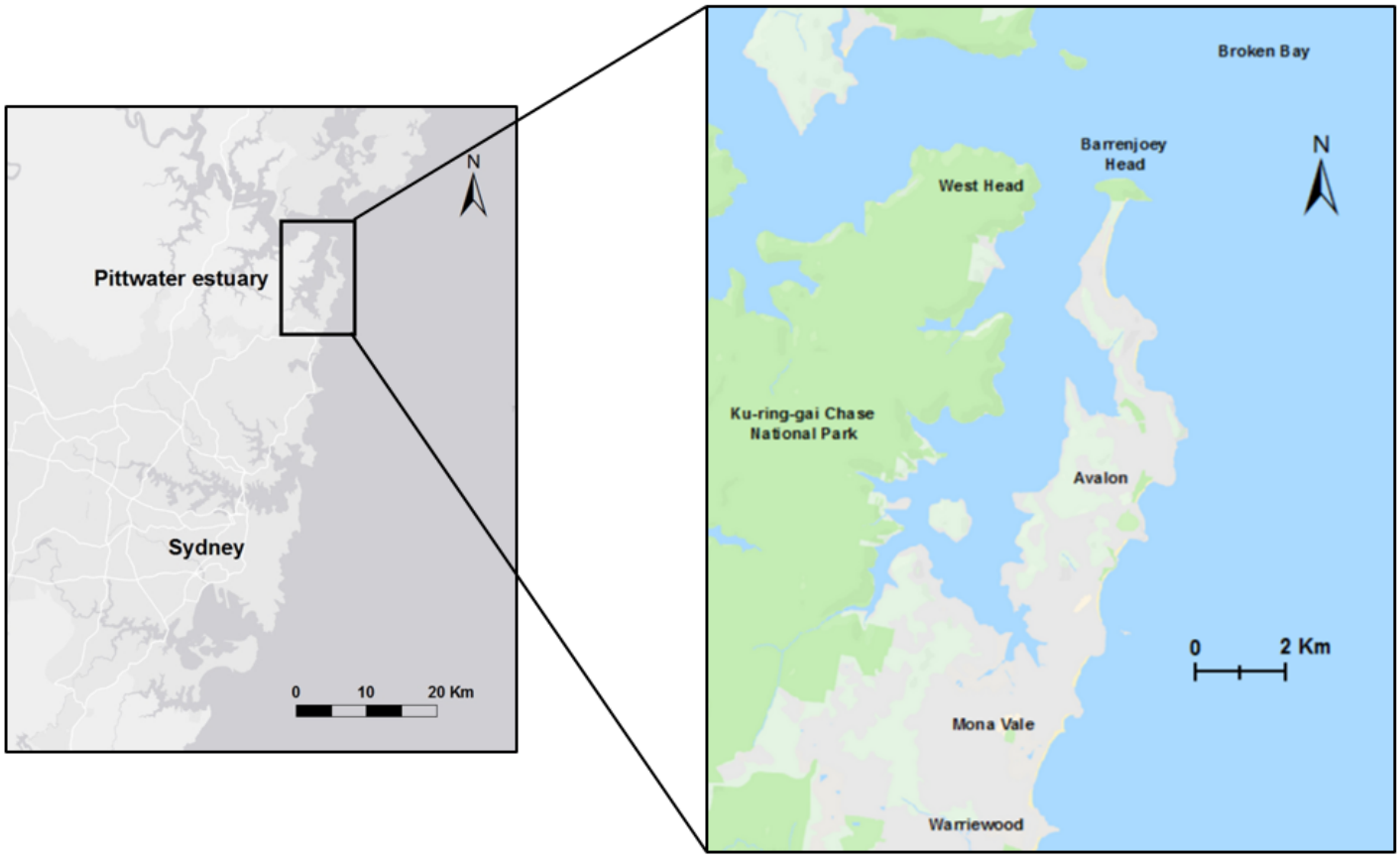

Figure 7: On the left panel, the Sydney area and on the right panel, the Pittwater estuary.
©ESRI Atlas for the left panel and Google Map for the right one

The Pittwater estuary is a drowned valley estuary in a semi-mature stage of evolution. It belongs to the group of the tide-dominated estuaries and have relatively steep slopes (Roy et al., 2001). Based on a report made by the NSW government (Roper et al., 2011), the Table 1 presents the physical characteristics of the Pittwater estuary:

Entrance Location	Latitude (°S)	-33.58
	Longitude (°E)	151.32
Catchment area (km^2)		50.8
Estuary area (km^2)		18.4
Average depth (m)		9.9
Estuary volume (ML)		181836.2
Perimeter (km)		56.2

Table 1: Physical characteristics of the Pittwater estuary.

3.1.1 History & Management

A summary of the history and management of the Pittwater area is given by Robert (2004). Prior to European settlement, the foreshores and headlands of the Pittwater estuary were inhabited by the Guringai tribe as the area would have provided an abundance of shellfish, fish and bush foods. In March 1788, Governor Philipp arrived in Broken Bay looking for land suitable for the cultivation of

food for a new colony (Pittwater Council, 2006). During this first expedition, he named the inland waterway "Pitt Water" after William Pitt the Younger, Prime Minister of Britain. From 1788 to 1900, the land remained mostly unoccupied. There were only a few fishermen, timber cutter, gardeners and the staff of the lighthouse. One of the reason of this low European activity was that the area was hardly accessible except by water. By the late 1920's, improvements were made on the roads and Palm Beach area became accessible to day trippers from Sydney which accelerated the development of the region (Pittwater Council, 2006). It quickly became a weekend and summer holidays destination. Nowadays, the metropolis of Sydney has extended to Palm Beach, Church Point and offshore communities in Pittwater.

The Pittwater waterway is one of the northern beaches natural assets and this waterway is under the pressure of multiple touristic, economic, recreational and social activities (Haines et al., 2008). To preserve the natural qualities of this place a sustainable management is required. Following the guidelines of the estuary management policy of of the New South Wales Government (NSW Government, 1992) and on behalf of Pittwater Council, a management plan for the Pittwater estuary has been finalized on August 2006. This plan contains goals and objectives for the future of the Pittwater estuary and will integrate and compliment the Lower Hawkesbury Estuary Management plan (Haines et al., 2008).

3.1.2 Studied beaches

The present study focuses on four beaches in the Pittwater estuary, selected to represent a variety of geomorphic settings in terms of exposure to swell waves due to varying distance from the inlet of the estuary and various aspects, shapes. Monthly topographic surveys have been undertaken at these beaches since May 2016. These four beaches are summarized below, where unless otherwise specified, information is from Short (2007) who documented environmental settings for all the beaches around Australia.

Figure 8: Location of the studied beaches and other key features. ©NearMap

Great Mackerel Beach

With a length of 640 m, Great Mackerel Beach is the longest beach of the western foreshore in the Pittwater Estuary. It consists of a narrow steep high tide beach that is partly protected from swell or wind waves. Moreover, this beach is sheltered from westerly winds by the escarpment of the Kuring-gai Chase National. Located at the northern end of the beach, a creek drains out and has built an inter-tidal sand shoals extending 200 m into the bay. In the centre of the beach is located a 60 m long jetty.

This beach takes its name from the fact that in the early days fishermen came there to capture their bait. Nowadays, this place is mostly used as wharf for residential boating activities. Note that there is no car access to this beach and it can be reached only by private boat or by the regular ferry that run from Snapperman Beach.

Figure 9: View of Great Mackerel beach from the southern part.

Sandy Beach

Sandy beach is located south of Sand Point and is 470 m long. This narrow high tide beach is backed by private properties with gardens. At the north-west end of the beach is a boat shed and slipway and further south-east are two jetties.

Before the 1960s, Sandy Beach and Snapperman were forming only one beach but, nowadays, they are no longer connected and are separated by 200 m of seawalls along Sand Point. According to a study made by Manly Hydraulics Laboratory (2012), past evolution of the shoreline at Sandy Beach indicates a long term accreting beach profile in the southern part of the beach. This can put the use of certain infrastructures at risk especially combined with the sea level rise. For example, constructions like the boat ramp will probably need some upgrades to maintain their serviceability in the future.

Figure 10: View of Sandy beach from the southern part.

Snapperman Beach

On the northern side of Sandy point begins Snapperman Beach which extends to Observation Point over a length of 640 m. On the northern part of the beach is located a boat shed as well as the public

Jetty from where the ferry that goes to Great Mackerel beach leave. Then, heading south, there is a large car park and many private homes.

Figure 11: View of Snapperman beach from the southern part.

Station Beach

Between the northern end of Observation Point and Barrenjoey Head stretch a popular recreational area for Sydney residents and tourists. This peninsula is two kilometers long and composed of an ocean beach, sand dunes, a vegetated backdune area and an estuarine beach. The latter is called Barrenjoey Beach or Station Beach and consists of a narrow (10 m) beach backed by minor dunes. The shoal that can extend up to 50 meters offshore is largely covered with sea grasses and shows typical depth of 2 to 5 meters.

Three distinct parts can be observed along the peninsula. Most of the residential development is in the south. The middle is mainly a recreational area with a golf course, Governor Phillip Park park and places for different water activities (swimming, surfing, sailing, etc.). The northern part of the beach consists of an heavily vegetated reserve.

Figure 12: View of Palm beach (on the left) and Station beach (on the right) from Barrenjoey Head.

As well as for previous beaches, Station Beach is affected by long period ocean waves that are heavily diffracted and refracted when entering Pittwater bay. They are hitting Station beach from the north-

north-west direction, causing southerly longshore transport. The beach is also affected by short period wind waves impinging the beach from direction between south and north-north-west causing northerly and southerly longshore transport (Australian Water And Coastal Studies, 1991). However, the zeta shape of the embayment and the beach cutback in the south of the jetty indicate a tendency for southerly longshore transport. The sand eroded from the beach is partly moved toward the south to Observation Point, from where a portion is transported further south to Snapperman Beach (Public Works Department, N.S.W, 1982).

Another important coastal process affecting this beach is offshore deposition. Indeed, during storms, the erosion of the beach face can lead to deposition of sand on the shoal, offshore from the beach. The other coastal processes like wind action on the dunes are believed to induce minor movements of sand compared to the other processes (Public Works Department, N.S.W, 1982).

3.2 Sites used for results comparison

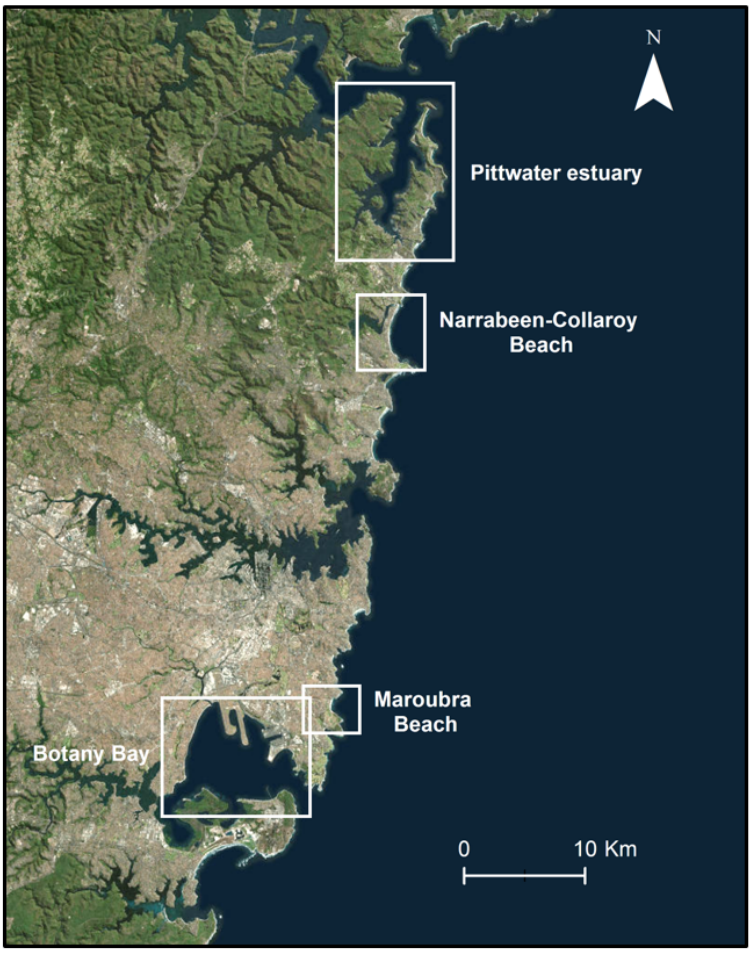

Figure 13: Location of the sites used to compare the post-storm recovery of beaches ©Google Map

3.2.1 Botany Bay

Located 15 km south of central Sydney, Botany Bay is an heavily urbanized coastal embayment that hosts Sydney's international airport and port. The decadal behavior of the beaches in Botany Bay

was analyzed by Schosberg (2017). Four sites within Botany Bay (Yarra Bay, Frenchmans, Congwong and Lady Robinsons beaches) are monitored with monthly profiling surveys using Real Time Kinematic GPS since May 2016.

3.2.2 Narrabeen-Collaroy Beach

Narrabeen-Collaroy is the second longest beach in Sydney metropolitan area with a length of 3.6 km. The beach faces east with wave height averaging 1.5 m at the northern part and less than 1 m in the southern part that is sheltered from the dominant southeast waves (Short, 2007).

Narrabeen-Collaroy is one of a limited number of sites where on-going and uninterrupted beach monitoring now spans multiple decades. Since 1976, five survey transects are monitored at monthly intervals. During the first three decades, profiles were surveyed using traditional survey techniques such as the Emery method. Since 2004, new and emerging survey technologies have been progressively implemented such as RTK-GPS, Lidar, coastal imaging and Unmanned Aerial Vehicles (UAVs) (Turner et al., 2016). The full Narrabeen Dataset is accessible online at http://narrabeen.wrl.unsw.edu.au/.

3.2.3 Maroubra Beach

Maroubra beach is the longest beach in the eastern suburbs of Sydney with a length of 1 km. The beach is oriented toward the east and thus very exposed to the waves generated in the Tasman Sea. Since 2006, Maroubra beach is recognized as a National Surfing Reserve because of the special place this beach has in Australia surfing history (Short, 2007). This beach as well as three other beaches in the eastern suburbs of Sydney are surveyed approximately every month since February 2016.

3.3 Oceanographic and meteorological conditions for Sydney area

This section will first present the ocean and wind conditions for Sydney area and then, in the next section, the focus will be put on the conditions that generate waves in the Pittwater estuary.

3.3.1 Hydrodynamic Data

A study of the wave climate for the Sydney region has been made by Short and Trenaman (1992). According to this study, ocean waves in this area are generated by *five meteorological systems* including three types of cyclones. *Summer tropical cyclones in the Coral sea* that generate moderate ocean swell waves with direction going from northeast to east, reaching Sydney 16 days per year on average. *Mid latitude cyclone in the Tasman Sea* generating moderate to low swell waves that reach Sydney during 200 days per year on average. The larger swell waves are generated by *east coast cyclones located in the northern Tasman Sea*, reaching Sydney 38 days a year on average (Short and Trembanis, 2004). Although the latter are not common, they are the greater contributor to flood and wind damage in this region. Moreover, they aren't easy to predict because of their relative small size and rapid development (Holland et al., 1987). Aside from cyclones, easterly swell waves can also be produced at any time of the year by *anticyclonic highs* and in summer *sea breezes* can generate waves from north-east sector.

The destructive power of severe cyclones, particularly when they occur coincidently with high tides and storm surge (the super-elevation of ocean levels associated with low atmospheric pressures and wind effects) may cause coastal inundation, beach erosion, damage to property and marine structures, and risks to public safety. High winds and intense rainfall which are often accompanying storm events can also cause damage.

To monitor the offshore wave climate of the Sydney coastal region, a non-directional Waverider buoy have recorded wave data from July 1987 to October 2000 and a directional Waverider buoy since the 3^{rd} March 1992. Wave height (H) and wave period (T) are available since July 1987 while wave direction (Dir) since March 1992. The location of the directional Waverider buoy is approximately 12 km east of Curl Curl beach at a depth of 92 m (see Figure 14). This buoy is maintained by Manly Hydraulic Laboratory (MHL) on behalf of the Office of Environment and Heritage.

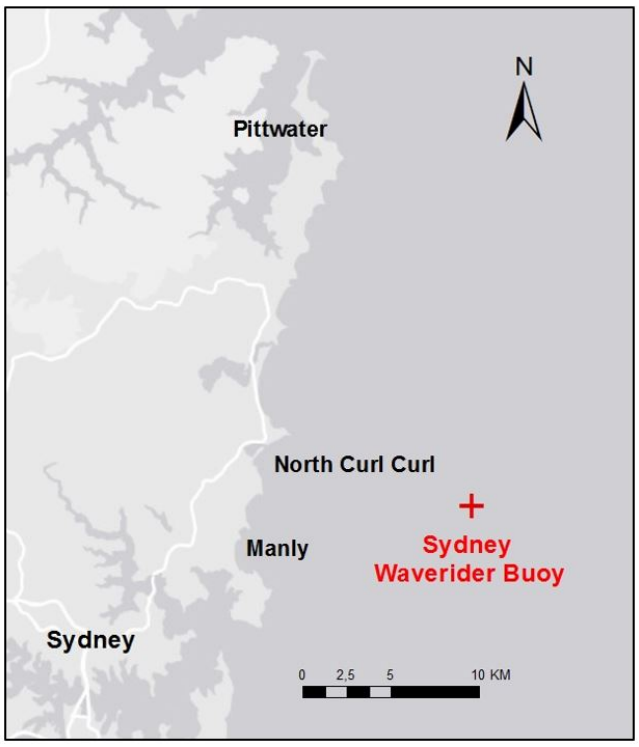

Figure 14: Actual location of Sydney Waverider Buoy. ©ESRI ATLAS

Hourly data from 17/7/1987 to 31/08/2017 were provided by MHL containing the following variables:

- H_{sig} [m] - The significant wave height corresponds to the wave height exceeded by 1/3 of waves per hourly interval. Wave height is the distance between the trough and crest of the wave.
- H_{max} [m] - The maximum wave height corresponds to the maximal wave height recorded during each time step.
- T_z [s] - The mean period of the waves for each time step. The wave period is the time for two consecutive crests to pass a fixed point. Longer waves period can be associated with more powerful waves.
- T_{P1} [s] - The peak spectral period corresponds to the wave period with the highest energy. The analysis of the distribution of the wave energy as a function of wave frequency is referred as spectral analysis.
- Dir [degrees] - The mean wave direction is defined as the mean of all the individual wave directions for a certain time step.

The overall mean significant wave height (H_s) is 1.63 meters, the overall mean period (T_z) is 6.17 seconds and the overall mean direction (Dir) is 135 degrees. According to Short and Trenaman (1992), a seasonal pattern is visible with longer period waves of moderate height during the winter, between April and September.

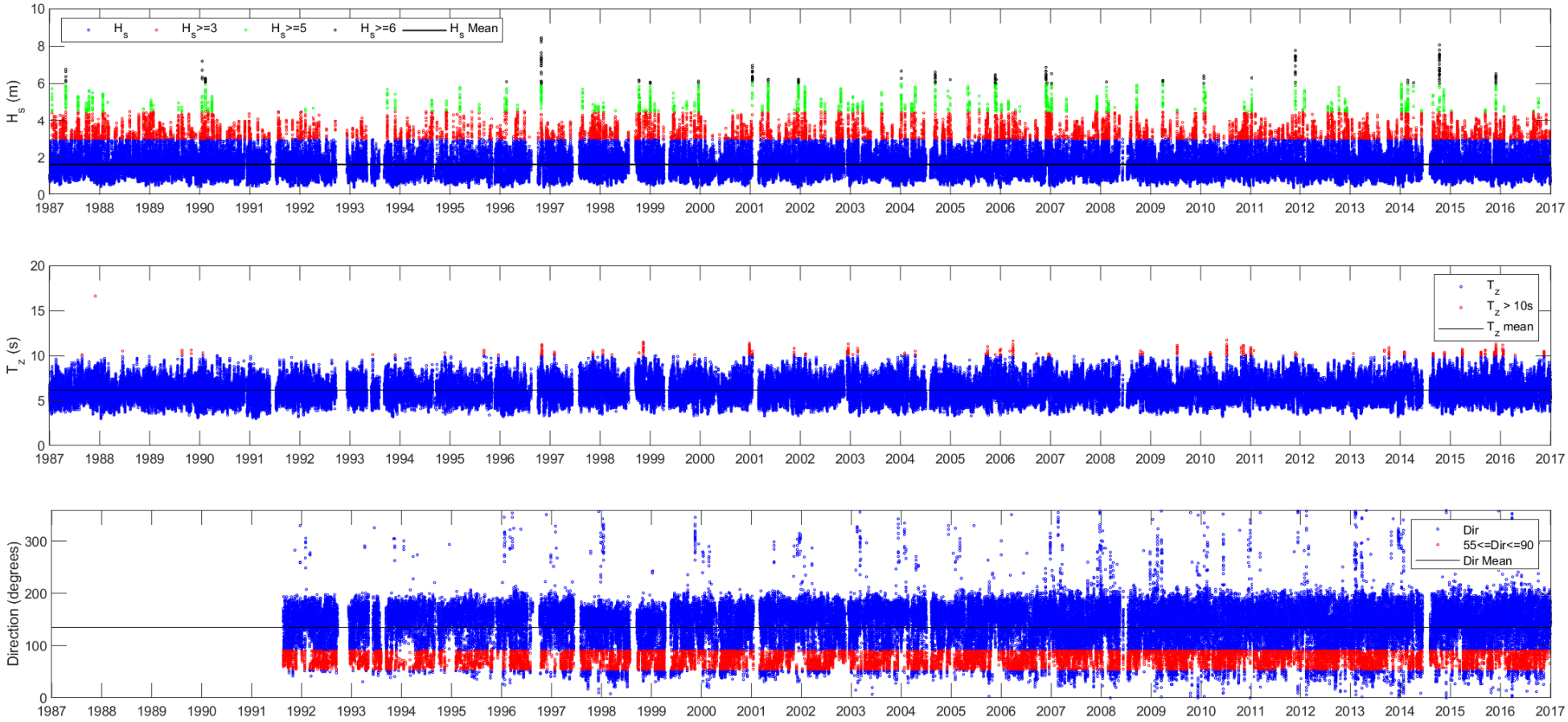

Figure 15: Wave heights greater than 3 meters as well as periods greater than 10 seconds for Sydney area since 1987 (in red). Waves direction between east-northeast and east are colored in red because the waves from these sectors are impacting mostly the Pittwater estuary as it is explained in the Section 3.4.1

3.3.2 Wind data

The closest governmental meteorological station from the Pittwater estuary is the Terrey Hills station, on the Hornsby plateau, at an elevation of 195 metres above sea level and belonging to the Australian Government Bureau of Meteorology. The town of Terrey Hills is located approximately 13 km southwest from the Pittwater estuary.

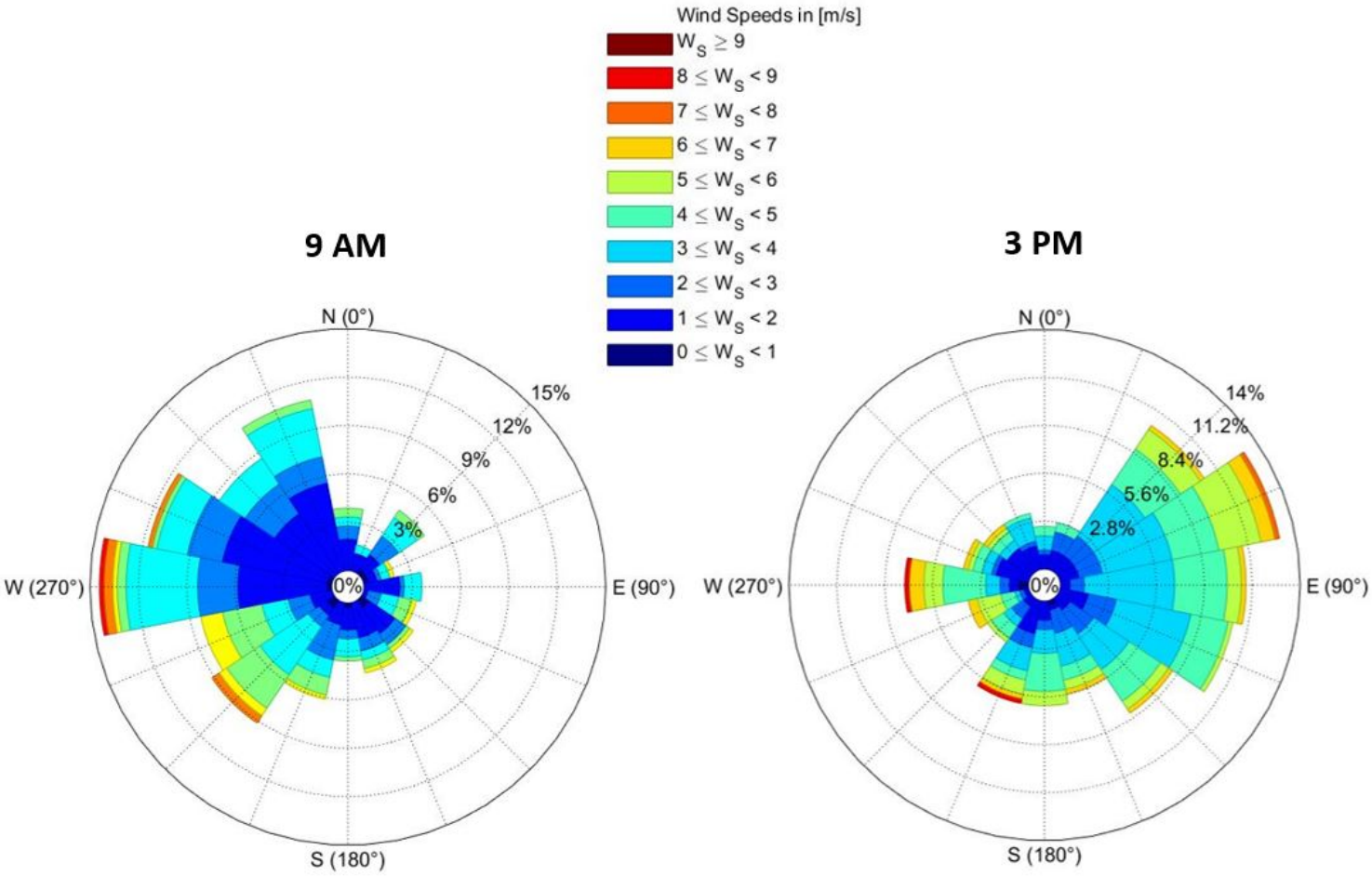

Figure 16: Wind roses for Terrey Hills, NSW - Average daily value from April 2017 to April 2018. Wind speed and direction are the average value in the last 10 minutes either before 9 AM or 3 PM.

The data are displayed in two wind roses attributing a percentage occurrence of winds within a set speed range. According to Figure 4, two wind direction are predominant at Terrey Hills, westerly and north-easterly winds. Westerly winds are predominant during winter while north-easterly winds are caused by late-morning to afternoon sea breezes active from spring to autumn, when the temperature differences between the ocean and nearby land is greater.

3.3.3 Tide data

The NSW coast has a mixed semidiurnal tidal cycle, resulting in two high and low tides per day that differ in height. According to Davies (1964), tide ranges can be classified as micro- (< 2 meters), meso- (2-4 meters) or macro-tidal (4-6 meters). The south-east Australian coast can be classified as micro-tidal. The mean neap tidal range that occurs just after the first or third quarter of the moon is around 0.79 m . The spring tidal range that occurs when the gravitational force of the moon and sun are combined and when the moon is full (or new) is 1.67 m. Solstice or "king" tide conditions

occur when the sun, moon and earth are aligned creating the most significant influence on the ocean water surface (Austin et al., 2009).

A tide-gauge was installed at Fort Denison in 1866 and since that year a continuous record of tides has been kept. However, data prior to 1914 have been considered unreliable, being affected by various errors making the records unreliable. Yet, hourly water level from 1914 to present are available providing an exceptional data record for Sydney Harbor (Watson and Lord, 2008).

3.3.4 Storm history

According to Shand et al. (2010), for the NSW coastline, an event of any duration with significant wave height greater than 3 meters recorded at an offshore wave recording station can be defined as a storm. Since July 1987, 12542 out of the 226575 hourly values recorded at the Sydney offshore station showed significant wave height greater than 3 m which corresponds to 5.73 % of the time. About 85 % of the mean direction assigned with these events was between south and south-east. Only 5 % of these storms generated waves with northeast to east direction.

In order to target the more powerful events that happened since 1987, storms with significant wave height greater than 5 m have been identified and are presented in Table 2. In the classification of coastal storms made by Shand et al. (2010) such events are characterized as major storms. During the period 1987-2017, 75 storms with significant wave height greater than 5 meters were detected by the offshore Sydney buoy. The wave direction of the majority of these events was from the south to south-east sector. Only 5 storms generated waves with direction from east to northeast. These storms have taken place in March 1995, July 1999, February 2004, March 2009 and June 2016.

Table 2: List of the major recorded storms (H_s > 5 $[m]$) - Data is from Sydney Waverider Buoy

Date	H_s **[m]**	*Direction*	**Duration with** H_s **>5 [hrs]**
03/08/1987	5,39	-	4
11/11/1987	5,65	-	21
09/02/1988	5,16	-	6
30/04/1988	5,33	-	6
25/05/1988	5,23	-	7
08/08/1988	5,30	-	7
25/07/1989	5,12	-	1
01/08/1990	5,12	-	2
03/08/1990	6,36	-	5
26/08/1990	5,75	-	15
13/10/1990	5,18	-	4
13/04/1994	5,41	S	6
10/06/1994	5,14	SSE	4
04/03/1995	5,10	ENE	2
18/06/1995	5,08	S	1
25/09/1995	5,52	SSE	6
19/08/1996	5,20	S	2
30/08/1996	5,41	SE	11
09/05/1997	6,21	SSE	49
07/03/1998	5,30	SSE	7
23/04/1999	5,58	ESE	16
28/04/1999	5,13	SSE	2
14/07/1999	5,49	E	15
29/12/1999	5,35	S	2
06/04/2000	5,03	S	1
30/06/2000	5,50	S	20
28/07/2001	6,18	S	19
19/11/2001	5,52	SSE	31
18/06/2002	5,03	SSE	1
29/06/2002	5,67	S	26
15/08/2002	5,36	SE	19
11/12/2002	5,16	ESE	2
04/05/2003	5,30	S	15
31/07/2003	5,27	S	2
11/10/2003	5,04	S	173
26/02/2004	5,44	ENE	3
18/07/2004	5,57	S	13
28/10/2004	5,47	S	12
22/03/2005	5,90	SE	16
24/06/2005	5,46	S	2
10/07/2005	5,71	-	2
15/11/2005	5,63	S	5
28/11/2005	5,27	S	2
07/02/2006	5,33	S	185
03/06/2006	5,84	S	21
11/06/2006	5,71	S	7
07/09/2006	5,09	SSE	164
08/06/2007	5,81	SSE	38
16/06/2007	5,58	ESE	4
20/06/2007	5,16	SSE	1
19/07/2007	5,58	SSE	12
05/11/2007	5,14	S	2
14/06/2008	5,16	S	5
23/08/2008	5,46	S	7
06/09/2008	5,06	SSE	154
31/03/2009	5,47	E	10
08/10/2009	5,75	S	12
03/08/2010	5,68	S	10
13/08/2010	5,35	SSE	6
20/07/2011	5,57	S	7
05/06/2012	6,44	S	22
11/08/2012	5,35	S	8
19/04/2013	5,27	S	6
02/06/2013	5,48	S	2
18/07/2014	5,10	S	20
18/08/2014	5,48	S	1
03/09/2014	5,01	S	11
14/10/2014	5,51	S	4
05/03/2015	5,83	S	2
20/04/2015	5,34	SSE	31
22/05/2015	6,68	S	8
05/06/2016	5,38	E	18
11/04/2017	5,93	S	2
19/08/2017	5,33	S	5
28/08/2017	5,38	S	4

3.3.5 List of exceptional storms events

The generally moderate wave climate of the south-east coast of Australia is periodically affected by large wave events originating from coastal storm systems. These very large storm event have strong impact on the coastline and, particularly when they are co-incident with high water levels, can cause large beach erosion, inundation and damage to property (Callaghan and Helman, 2008). Since one of the objective of this study is to identify long term shoreline changes, the larger storms that occurred during the last decades are presented here.

- 1974 -

The character of many beaches along the central and southern coast of the New South Wales changed after three periods of strong erosive wave conditions during May 24th and June 18th (Bryant and Kidd, 1975). It was qualified as one of the three most severe storms that hit the Sydney coastline since white settlement (Callaghan and Helman, 2008). The return period of this storm is around 100 years and is generally used as reference for storms design (Lord and Kulmar, 2001). Moreover, it is after these storms that a network of Waverider buoys and water level recorders along the New South Wales east coast was installed.

- 1997 -

The "Mother's Day" storm is the largest storm on record. It happened in May 1997 and the storm peaked during the night of the 10th-11th May, with a significant wave height reaching 8.43 m at both Sydney and Port Kembla and 8.86 m at Botany Bay (Shand et al., 2010).

- 2007 -

In June 2007 occurred the largest storm event by total storm power, the "Pasha Bulker Storm". The peak height was not extremely high with 6.90 meters in Sydney but it remained elevated over 3 m for 8 days and over 5 m for nearly 2 days which leaded to major flash flooding, massive coastal erosion and over 1.5 billion $ in damage costs (Mills et al., 2010).

- 2016 -

In June 2016 an unusual East Cost Low created a large and relatively stable north-easterly fetch directed at the coastline for several days (Harley et al., 2017a). Most open ocean beaches of the eastern seaboard of Australia experienced the worst erosion in 40 years. The major determinant of this erosion magnitude is the east to north-east storm wave direction as well as the coincidence with winter solstice spring tide. Indeed, easterly wave direction partly avoid the energy attenuation across the continental shelf and focus wave energy on coastal Section not equilibrated under the prevailing south-easterly wave climate (Mortlock et al., 2017).

During the last decades, the apparent frequency and storm damage have increased while there is no discernible change in frequency of occurrence or severity of storms. According to Public Works Department, N.S.W (1986), this is linked with the rapidly growing population and urbanization of the coast but also because of the long term recession of the coastline increasing the exposure of the constructed assets.

3.4 Wave climate in the Pittwater estuary

Wave conditions in the Pittwater estuary are generated from two main sources : locally generated wind waves and ocean waves penetrating through Broken Bay (Australian Water And Coastal Studies, 1991). Also, noteworthy, waves can also be generated by the boat activity in the estuary. Yet, according to the study done by Australian Water And Coastal Studies (1991), they are not powerful enough to generate significant sand transport.

3.4.1 Ocean generated waves

Ocean waves that enter the estuary are not as high as on open ocean beaches. This is because of the energy dissipation caused by shoals in the estuary entrance and the process of diffraction and refraction undergo by the waves when they penetrate the estuary (Jackson, 1995). The proximity from the entrance of the estuary as well as the orientation of the beach will define the reduction factor.

A wave transformation model was established by Australian Water And Coastal Studies (1991) to estimate the heights of the offshore waves penetrating the Pittwater estuary, for different offshore wave directions. Wave height reduction factors were calculated taking into consideration wave refraction, diffraction, shoaling and frictional losses. The sensor used to determine empirical coefficients was deployed from August 1988 to October 1989 at Great Mackerel public wharf and at the Sydney offshore Waverider buoy station.

Table 3: Offshore Wave Coefficients - From the wave transformation model established by Australian Water And Coastal Studies (1991)

Offshore Wave Direction	Station Beach	Snapperman Beach	Sandy Beach	Great Mackerel Beach
NNE	0	0	0	0
NE	0.04	0.06	0.03	0.16
ENE	0.11	0.17	0.07	0.22
E	0.14	0.18	0.07	0.26
ESE	0.05	0.06	0.01	0.16
SE	0.04	0.05	0.01	0.08
SSE	0.02	0.04	0.01	0.04
S	0	0	0	0

In Table 3, the values correspond to the ratio between inshore wave heights and offshore wave heights. Offshore waves from sector east to east-northeast generate the highest waves in the estuary and Mackerel beach is more impacted by swell waves that the others beach in the northern part of Pittwater. However, as seen in Section 3.3.4, during the period 1987-2017, only 5 out of a total of 75 major storm events showed waves direction from the east to northeast sector.

3.4.2 Locally Generated Wind Waves

The second type of waves to consider when studying embayed beaches is wind waves generated locally inside the estuary. Wind wave generation is governed by a limited set of parameters such as wind fetch (uninterrupted distance of open water over which the wind blows without significant change in direction), water depth, wind velocity and bottom friction.

Table 4: Locally Generated Waves in the Pittwater estuary studied beaches - From the model established by Australian Water And Coastal Studies (1991)

	Maximum Av. Fetch [m]	Direction	Return Period					
			20		50		100	
			H_s [m]	T_p [s]	H_s [m]	T_p [s]	H_s [m]	T_p [s]
Station Beach	3077	SW	1.2	3.2	1.4	3.3	1.5	3.4
Snapperman Beach	3129	N	1.2	3.2	1.4	3.3	1.5	3.4
Sandy Beach	-	-	-	-	-	-	-	-
Great Mackerel Beach	2160	SE	1	2.8	1.1	2.9	1.2	3

The significant wave height (H_s) and peak spectral wave period (T_p) shown in the Table 4 were calculated using a computer model developed by Australian Water And Coastal Studies (1991). Wind speeds of 28.1 $[m/s]$, 30.8 $[m/s]$ and 32.9 $[m/s]$ for respectively 20, 50 and 100 years return period were used to establish the model. This procedure aimed to calculate the maximum heights of locally generated wind wave heights for each site. The results indicate that with its elongated shape, large wind waves can be generated inside the Pittwater Estuary, particularly impacting the beach located in the eastern part of the estuary.

A point that is not taken into account in the two previous chapters is that both conditions can take place at the same time. Moreover, if this is combined with strong tides, it can have important consequences on the morphology of the beaches studied.

4 Methods

4.1 Decadal evolution

The analysis of the long term shoreline displacement was conducted along three transects located in the northern, middle and southern part of each studied beach. They are labelled according to the profile names of the surveys because of their common origin (see Figure 17). For this analysis, the number of transects has been limited to three in order to facilitate the comparison between the different sectors.

Figure 17: Location of the transects for the shoreline analysis.

4.1.1 Source of images

The long term changes in beach width was investigated using aerial photographs and satellite images. A great collection of aerial photographs for the state of the New South Wales can be found at the Office of Environment and Heritage in Newcastle where a scanner is available for digitization. The resolution of these images vary according to the years and are not always specified. The scale ranges from 1:42000 for the oldest images to 1:4000 for the more recent.

Table 5: Available aerial photographs that cover the northern part of the Pittwater Estuary

Date	Capture scale	Covered Area			
		Great Mackerel Beach	Sandy Beach	Snapperman Beach	Station Beach
29 Sep. 1940	1:32000	x	x	x	x
1941	-	x			x
01 Jan. 1947	-	x	x	x	x
01 May 1951	-		x	x	x
02 Dec. 1951	1:42000	x	x	x	x
30 Apr. 1952	1:18000		x	x	x
28 Sep. 1955	-	x	x	x	x
09 Jul. 1961	1:45000		x	x	x
18 May 1962	1:18000		x	x	x
23 Sep. 1965	-	x	x	x	x
28 Aug. 1970	-	x	x	x	x
19 Jun. 1974	1:16000		x	x	x
16 Nov. 1976	1:16000	x	x	x	x
22 Dec. 1977	1:4000				x
02 Aug. 1978	1:4000				x
14 Apr. 1979	1:4000				x
20 Jul. 1979	1:6000		x	x	x
28 Mar. 1980	1:8000		x	x	x
03 Mar 1981	1:10000		x	x	x
09 Jan 1982	1:8000		x	x	x
20 Aug. 1982	1:16000		x	x	x
30 Mar. 1983	1:8000		x	x	x
01 Apr. 1985	1:16000	x	x	x	x
18 Aug. 1986	1:8000	x	x	x	x
10 Mar. 1988	1:16000	x	x	x	x
04 May 1990	1:8000	x			
18 Aug. 1990	1:6000		x	x	x
19 Apr. 1993	1:6000	x	x	x	x
30 May 1996	1:6000	x	x		x
20 May 1999	1:6000		x	x	x
13 Sep. 2001	1:6000				x
22 Apr. 2004	1:8000	x			
03 Jul. 2008	1:10000	x	x	x	x

The satellite images used are from two different sources, DigitalGlobe (https://www.digitalglobe.com) and NearMap (https://www.nearmap.com.au) companies. The resolution of these images range from 0.6 m for the NearMap images to 1.2 m for the DigitalGlobe images, depending on the chosen canals.

To investigate the long term stability, since the interval between the images should not be too short to avoid aliasing effects (see Section 4.1.3), not all the available aerial or satellite images were used. The images on which the shoreline identification is complicate were left behind. The Figure 18 summarize the images used for the investigation of the long term stability. For each beach, the detailed list of images used can be found in Appendix 1.

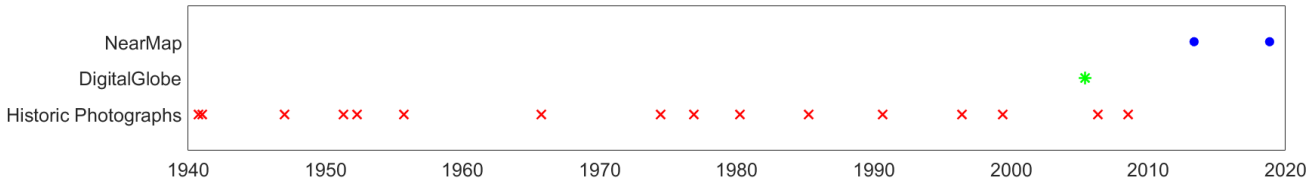

Figure 18: Date and source of the images that have been used to assess the decadal evolution of the shorelines.

4.1.2 Image georeferencing

The scanned photographs were first re-sized to fit the area of interest in order to facilitate and improve the accuracy of the georeferencing processes. Second, they were rectified in ArcGis using a satellite image from NearMap as base map, already projected in the Universal Transverse Mercator (UTM) coordinate system. A summary of the methods used for transformation of remotely sensed data is given by Novak (1992). The most common transformation use polynomial functions that are defined using ground control points (GCPs) that have to be identified on the scanned photographs and on the base map. In general, GCPs are landmarks such as large rocks, corners of buildings, road intersections, etc. The size of the image as well as the availability of easily identifiable features control the requisite number of control points. In the present study, their amount ranged between 10 to 25 (a minimum of 7 points is required to perform a polynomial transformation of 2nd degree).

The polynomial rectification is then based on a curve fit where the maximum exponent corresponds to the degree of the polynomial function. The original image will be stretched, scaled, rotated, bent and curved to fit best to the control points chosen. According to Rocchini et al. (2012), it's rare to go beyond a second degree transformation because higher degree polynomial or spline function will provide a perfect fit at the reference points but due to undulations between these points, large errors can be present outside the GCP range. Polynomial function cannot correct relief distortion because it only take into account the x and y coordinates of the GCP but not the elevation. When the elevation is taken into account, the process is called differential rectification or ortho-rectification Rocchini et al. (2012). Since the relief distortion is not really important in our study area (mean elevation of the studied beaches is around mean sea level), the relief distortion has not been taken into account. However, a special attention was paid to not place GCPs on elevated area.

The accuracy of the rectification is estimated by the root mean square error (RMSE). The RMSE corresponds to the sum of all the residuals which refer to the distance between the location specified for a control point and the place where he ends up after the transformation of the original image Rocchini et al. (2012). The RMSE is a good indicator of transformation accuracy and should not be too large. However, even is the RMS is close to zero, it doesn't mean that the image will be perfectly georeferenced, especially when using higher degree polynomial that can lead to important errors outside the GCP range. In the present study, RMSE values obtained for the rectification process were between 0.5 to 5 m, depending principally on the quality of the GCPs and on the scale of the image (see Appendix 1 for the RMSE values of the different rectified images).

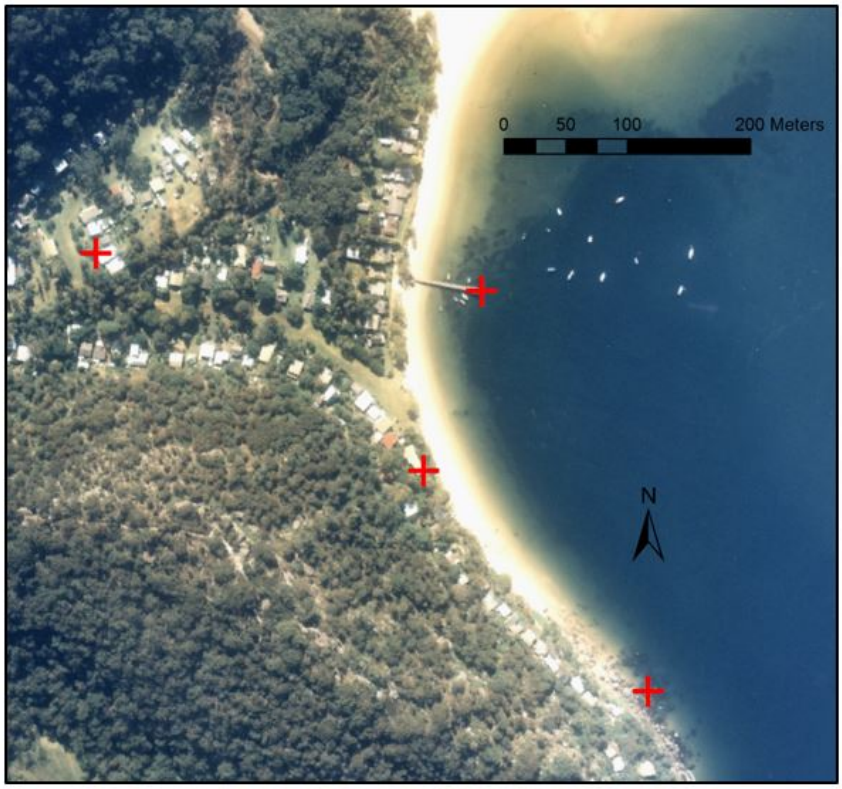

Figure 19: Example locations of ground control points used for the rectification of aerial photographs - Great Mackerel Beach

4.1.3 Shoreline interpretation

To investigate long term shoreline stability, the principal methodology approach is to draw the shoreline position from the data sets available (aerial photographs, satellite images, contour maps). However, first, it is necessary to choose to which feature corresponds the shoreline. According to Boak and Turner (2005), an idealized definition of the shoreline is the physical interface between the land and water. On an aerial or satellite image, this limit may be visualized as the edge of the dark water body, a foam line or by a line of specular reflection from the edge of the dark water body (Shoshany and Degani, 1992). However, opting for this definition of the shoreline raise some problems, first the foam line does not always correspond to the water line and second, the resolution of the photographs is often not small enough to properly see the edge of the water body. Finally, the water limit changes continuously over time because of the dynamic nature of the water level (tides, waves, groundwater, etc.) and the sediment movement.

An alternative line must be chosen and the high water limit is the most common shoreline indicator for historical shoreline comparison (Hanslow, 2007). It should be noted that the term High Water Line (HWL) is often confused in the literature and this point deserve some clarification before going any further. The definition used in the present study is the same than the one used by McBride et al. (1991) ; the HWL corresponds to the location of the wet and dry beach contact that usually represents the non-storm high tidal wash of the waves (Crowell et al., 1991). This feature can be identified on aerial images because of the change of tone between the wet and dry sand. The HWL is also more stable in time than other features because of the rate at which the sand dry. However, in cases where the resolution of historical photographs is too low to visually identify the wet-dry line, the shoreline feature chosen in the present study is the zone of high-pixel brightness variance

(Shoshany and Degani, 1992). The use of some alternatives lines such as high tide line, berm line was examined but it was found that the high water line is offering better stability and detectability in this case.

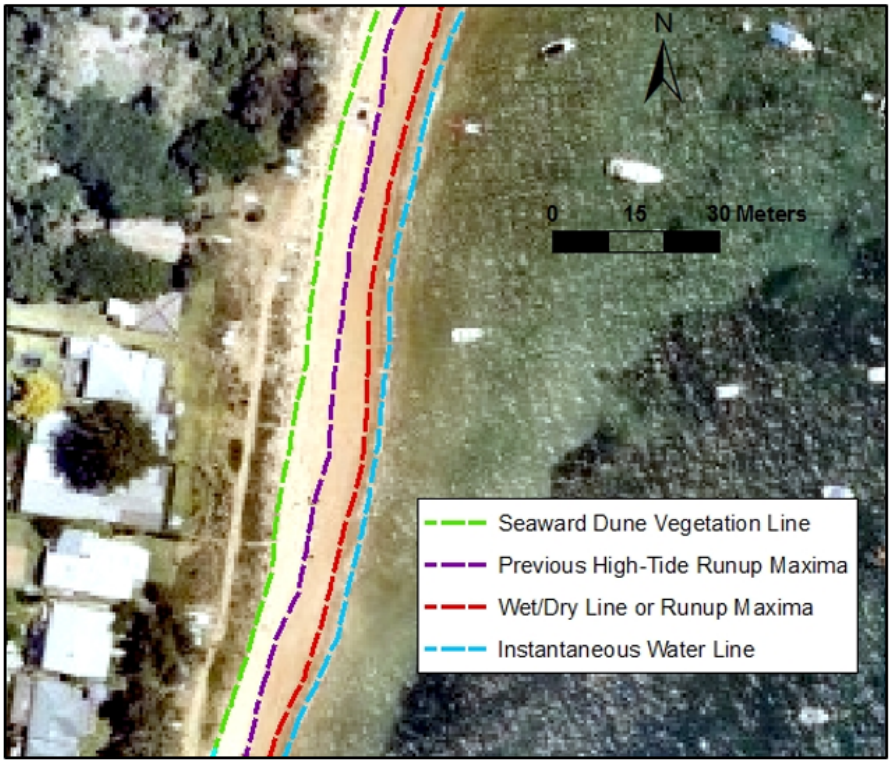

Figure 20: Example of visibly discernible shoreline features on an aerial photographs of Mackerel Beach. The shoreline feature used in this study is the High Water Line also referenced as wet/dry line or runup maxima

4.1.4 Uncertainties

The uncertainties and errors associated with shorelines extracted from aerial photographs and satellite images need to be taken into account when studying shoreline changes. The total uncertainty estimation is a good indicator of the minimum shoreline change signal that can be reliably investigated by studying shoreline displacement (Ruggiero et al., 2003). However, quantifying measurement error is probably one the most difficult step of long term shoreline measurement (Smith and Zarillo, 1990). In short, the total uncertainty of shoreline position is a combination of source accuracy, interpretation error and natural short term variability (Ruggiero et al., 2003).

Source accuracy is related to the fact that the High Water Line on aerial photographs is not always easily discernable. Sometimes, it is because the quality of the source media is too low to be able to identify the shoreline feature properly. This depend of the camera used and the altitude at which the images were taken. It can also be the case when the photo is taken just prior or after the high tide or after a rainy event because the wet-dry sand limit is nonexistent. Moreover, if the angle between the ground and the camera is too high, the reflectivity will mask the difference in shading (Ruggiero et al., 2003).

Another inherent source error associated with aerial photographs is the rectification of aerial images. For this factor the RMSE is a solid estimator. As seen in Section 4.1.2, the RMSE ranged between 0.5 and 5 m (see Appendix 1). An average value for the uncertainty related to georeferencing was estimated to be around $\pm$ 2 m.

Shoreline interpretation error corresponds to the difference of shoreline position after several repeated digitization. It is mainly related to the skill of the operator doing the operation. In the

present study, this factor has been minimized by doing a detailed description of the shoreline feature to identify (see Section 4.1.3) and because the digitization of the shoreline was always made by the same operator. From repeated shoreline digitization of the same coast by a single operator, Fletcher et al. (2003) found that the mean difference between shoreline position was $\pm$ 3 m and Ruggiero et al. (2003) found a difference in shoreline position of $\pm$ 2 m.

Short term variability also called positional uncertainty by Fletcher et al. (2003) is by far the largest uncertainty. It is caused by features and phenomena that influence the shoreline position at the time of the aerial photograph or satellite image was collected. It can be linked with the short time scale variability of the beach morphology or to other phenomenon like tidal fluctuation, changes in wave run-up, seasonal beach recovery or change in the angle of wave incidence (Ruggiero et al., 2003).

Except during storms event, the total water level in tidal estuarine beaches such as the Pittwater estuary is mostly affected by tidal fluctuation (Australian Water And Coastal Studies, 1991). For this reason, the positional uncertainty is associated with the tidal fluctuation causing horizontal displacement of the water line. It can be quantified using the mean spring tidal range that equals 1.25 meters for the Sydney area (Manly Hydraulics Laboratory, 2015) and the mean slope of the beach that is approximately 10 degrees according to the beach surveys results. This lead in an horizontal displacement of around $\pm$ 6 meters. Ideally, in order to minimize the short term variability, aerial images should be taken at the same tidal level and during period of the year with low wave climate Ruggiero et al. (2003).

Table 6: Uncertainties related to positional and measurement errors

Source	**Magnitude**
Onscreen delineation	$\pm$ 3 $[m]$
Orthorectification and source accuracy	$\pm$ 2 $[m]$
Short term variability	$\pm$ 6 $[m]$
Total Uncertainty	$\pm$ **7** $[m]$[1]

[1]Calculated as the root sum squared of the individual uncertainties

To overcome the short term variability and be able to observe some long term trends, the interval of time between the images chosen should not be too short. Ideally, it should be long enough to establish a significant net change in shoreline position that is greater than the short term variability (Smith and Zarillo, 1990). In the present study, the time interval between aerial photographs ranges from 5 to 10 years.

Another solution to reduce the short term variability would be to use less dynamic shoreline features like the erosion scarp or the vegetation line but these features are not always clearly defined and can be affected by man modification like those resulting from leveling for development purposes or sand extraction. Moreover, the vegetation line is cultivated on most part of the developed beaches of the Pittwater Estuary and does not represent the natural movement of the shoreline. Another point it that using these morphological features is case specific because they are good indicators of erosion but may not show accretion or will show it with a significant time lag because of the longer recovery time (Boak and Turner, 2005).

4.2 Monthly to seasonally changes

Long term data sets like aerial photographs allow to study decadal shoreline changes but to investigate the monthly to seasonally evolution of a beach, small scale data sets are preferred because of the better accuracy and objectivity that they provide (Ruggiero et al., 2003). Different methods can be use to collect such data but the basic form of beach morphology monitoring aims to obtain cross-shore beach profiles that are perpendicular to the shoreline.

A variety of survey methods can be used to obtain beach profiles. One of the older technique is the one proposed by Emery (1961) that use two graduated rods to determine the difference of elevation along a beach profile. More sophisticated methods such as LiDAR (Light Detection And Ranging), RTK-GPS (Real Time Kinematic Global Positioning System) or unmanned aerial vehicles (UAVs) allow faster data collection at higher resolution that can generate three-dimensional representations of beach morphology (Harley et al., 2011).

4.2.1 Topographic Survey

Since the 20^{th} May 2016, topographic surveys using RTK-GPS are performed on the four study sites in the Pittwater Estuary every 1-2 months. A total of 20 beach surveys campaigns were performed between May 2016 and June 2018. For each beach, five or six cross-shore profiles are surveyed by walking perpendicular to the contours, from the datum points towards the shoreline and into shallow water (see Figure 21). Except for Station beach, long-shore measurements are also performed along the entire length of the beaches, by zigzagging between the shoreline and the dune crest. Elevation and location data ($x_{gps}, y_{gps}, z_{gps}$) are logged every meter. To reduce measurements errors, the measuring device should be held as vertically as possible and with the lower part as close to the sand as possible.

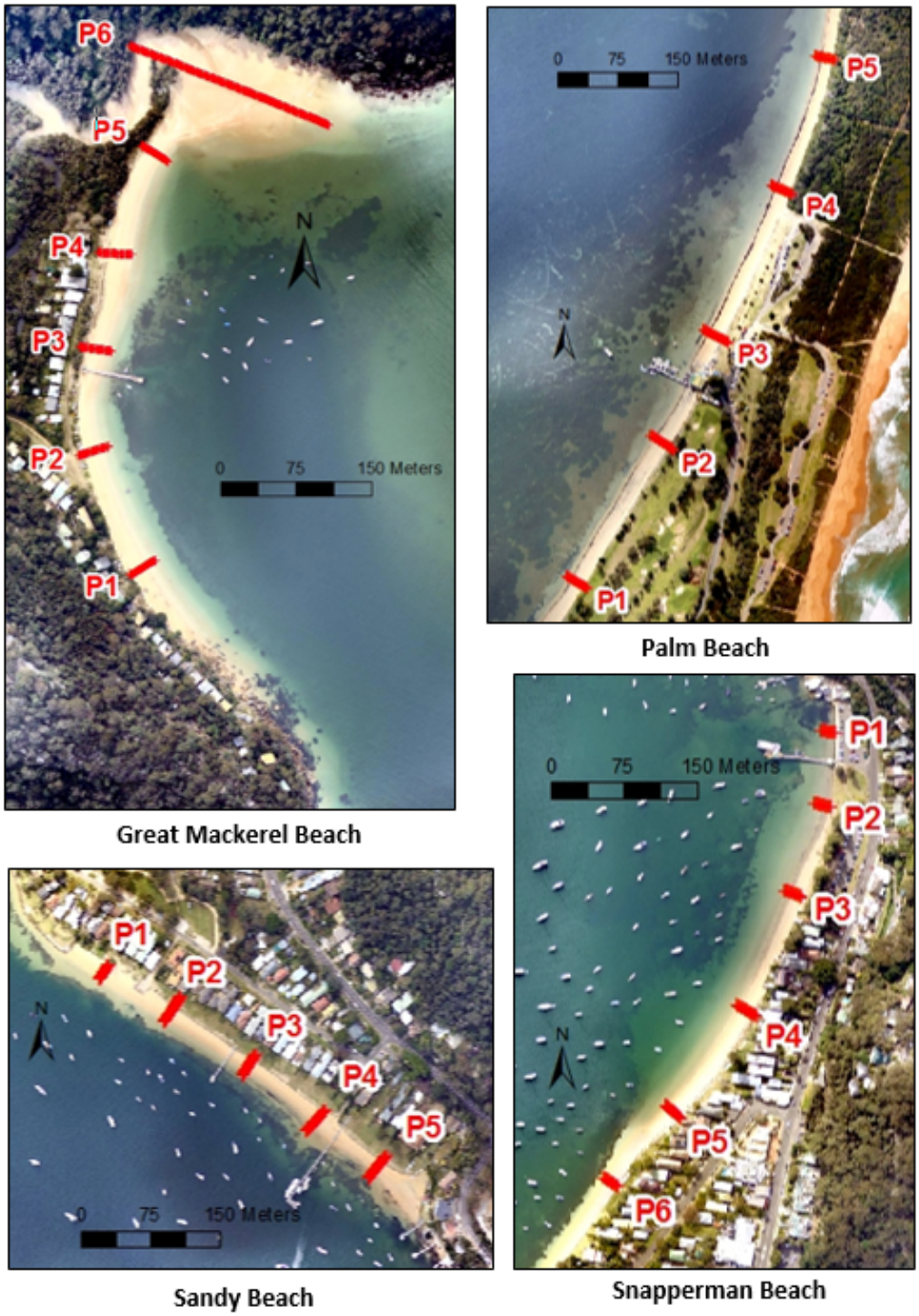

Figure 21: Location of the RTK-GPS survey profiles

Individual profile can provide information about cross-shore morphology and allow to derive beach height, width and gradient. Long-shore profiles give information about beach volume and three dimensional features. Profiling must be done regularly to capture monthly changes and during a long enough period of time to obtain meaningful time series (Short and Trembanis, 2004). In comparison with aerial photographs analysis, GPS-surveys doesn't rely on subjective visual interpretation and allow for a more objective and repeatable datum-based estimate of shoreline position (Ruggiero et al., 2003).

4.2.2 Calculation of the width, slope and volume

For each profile, the width was calculated from the profile origin to where the profile reach mean sea level. When necessary, horizontal adjustments of the profile origin were made so that the origin corresponds to the foredune crest. The slope was calculated as the altitude difference between the origin point and the mean sea level divided by the beach width. The subaerial volumetric area $[m^3/m]$ was calculated for each profiling survey that were carried out using a trapezoidal function on Matlab. The seaward limit corresponds to the mean sea level and the landward limit corresponds to the dune crest.

To investigate the post-storm recovery of the studied beaches, the method used in the present study is similar to the one proposed by Harley et al. (2017b) that studied the recovery of Narrabeen-Collaroy Beach after June 2016 storm. The difference of subaerial volume between two dates $[m^3/m]$ is calculated for each transect using the following equation :

$$\partial V = \int_{x_0}^{x_d} (z_1)\, dx \; - \; \int_{x_0}^{x_d} (z_2)\, dx \tag{1}$$

where x_d is the origin point corresponding approximately to the position of the dune crest, x_0 is the cross-shore position of the mean sea level contour ; z_1 and z_2 are the elevation data for the two dates of interest. The integral is calculated using a trapezoidal function on Matlab. Then, the percentage of volume recovery for a given period of time is calculated using the following equation :

$$\%recovery = 100 \cdot (1 - \frac{\partial V_{recovery}}{\partial V_{storm}}) \tag{2}$$

where ∂V_{storm} correspond to the difference of volume directly before and after the storm while $\partial V_{recovery}$ correspond to the difference of volume before the storm and after a given period of time.

5 Results

5.1 Decadal evolution

Long term fluctuations of beaches in time are categorized under two processes; seaward migration of the shoreline is called beach accretion, and landward movement is called recession. This is driven by sediment transport, due to variations in meteorological and hydrodynamic forcing including wind, waves, sea level and currents.

The Figure 22 on the following page presents the long term evolution of the studied beaches. The results are summarized in the Table 7 below.

	Annual change rate $[m/year]$			Total change between 1941 and 2017 $[m]$		
	Northern	Middle	Southern	Northern	Middle	Southern
Station beach	-0.01	-0.04	-0.01	-3	-2	1
Snapperman beach	-0.13	-0.10	-0.11	-11	-6	-4
Sandy beach	-0.10	0.07	0.33	4	12	29
Great Mackerel beach	-0.28	-0.13	-0.34	-19	-5	-24

Table 7: Shoreline changes from 1941 to 2017. On the left table, the annual rate of change is calculated along each transect using the slope of a linear fit to the time series of shoreline positions. On the right panel, the total change is the shoreline displacement between the year 1941 and 2017. A negative rate means that the beach has been eroded during the study period while a positive rate means that the beach has been accreting

Station Beach

As illustrated on Figure 22a, Station Beach remained relatively stable over the study period. The total long term changes of the shoreline position is small as well as the annual change rate (see Table 7). Concerning the longshore variability, the three parts of the beach behaved in a similar way.

In the 1980s, another investigation of historic photographs of Station Beach and Palm Beach has been made for the period 1940-1978 (Public Works Department, N.S.W, 1982). They found a recession rate for Station beach up to 0.35 $[m/year]$. Their results strongly differ from the annual change rate found by the present study that is close to zero $[m/year]$ (see Table 7). Since the period of time covered by their study is not the same, this difference is probably linked with the natural beach evolution that alternate between period of recession and accretion. On Figure 22a, this phenomenon is visible with the period between the 1940s and 1974 that show erosion, followed by a period of accretion between 1974 and the end of the 1990s. Then, during the last two decades, the beach is narrowing again.

Snapperman Beach

The width of Snapperman beach has slightly decreased between 1941 and 2017 (around 10 m). There is no noticeable difference between the different areas of the beach. The northern, middle and southern areas have followed a similar trend.

Similar as for Station Beach, the effects of the 1974 storm are visible on the Figure 22b. The storm coincide with a decrease of the beach width and is followed by a period of accretion.

A : Station Beach

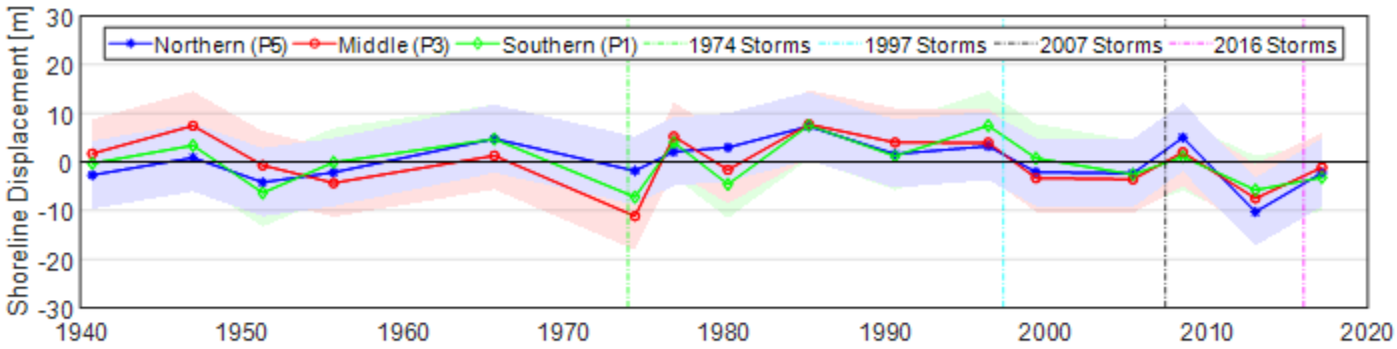

B : Snapperman Beach

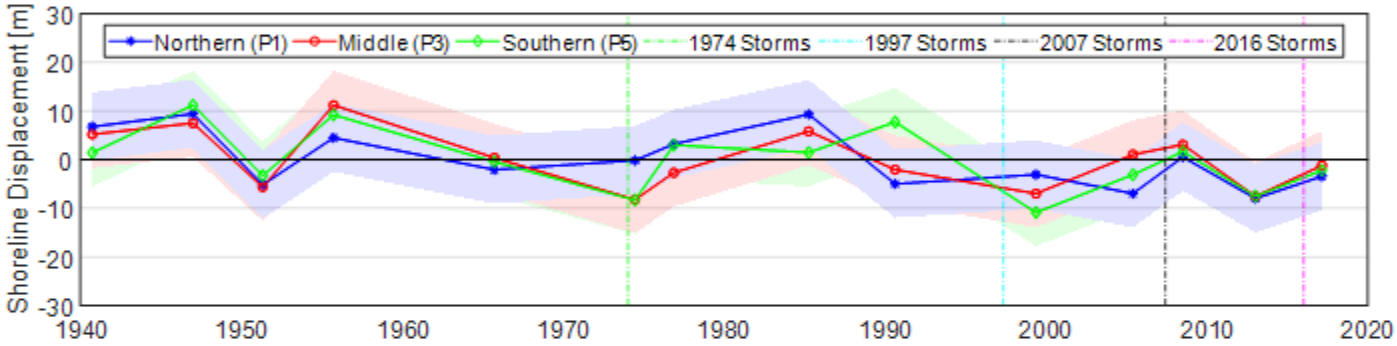

C : Sandy Beach

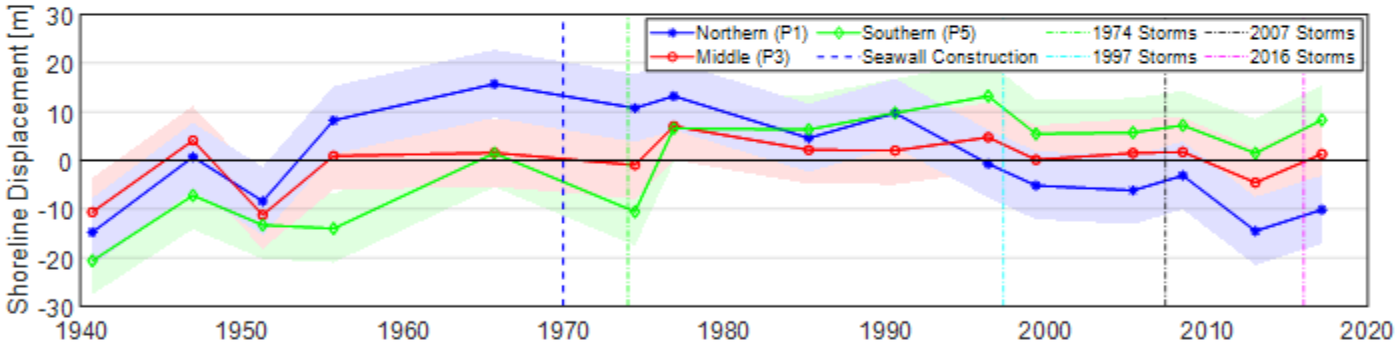

D : Great Mackerel Beach

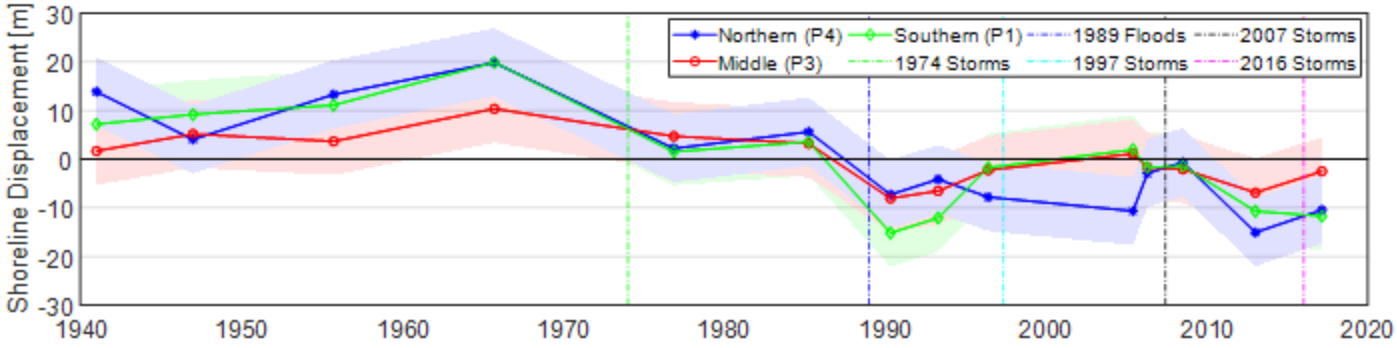

Figure 22: Shoreline displacement for the period 1941-2017 represented with the uncertainty associated (see Section 4.1.4). The distance between the shorelines and the reference point are centered around the mean distance value to easily visualize accretion and recession periods. The dashed vertical lines represent the four larger storms that happened during this period of time (see Section 3.3.5).

Sandy Beach

Unlike the two previous beaches, important changes happened in Sandy Beach since the 1940s. First, until the 1980s, the beach accreted along its entire length, with a shift of the shoreline of about 20 m. Second, since 1980s, the southern part of the beach continued to grow whereas the northern part began to erode. On Figure 23, this clockwise rotation of Sandy Beach is clearly visible at both extremity with a difference of about 15 m between the shoreline in 1974 and in 1999.

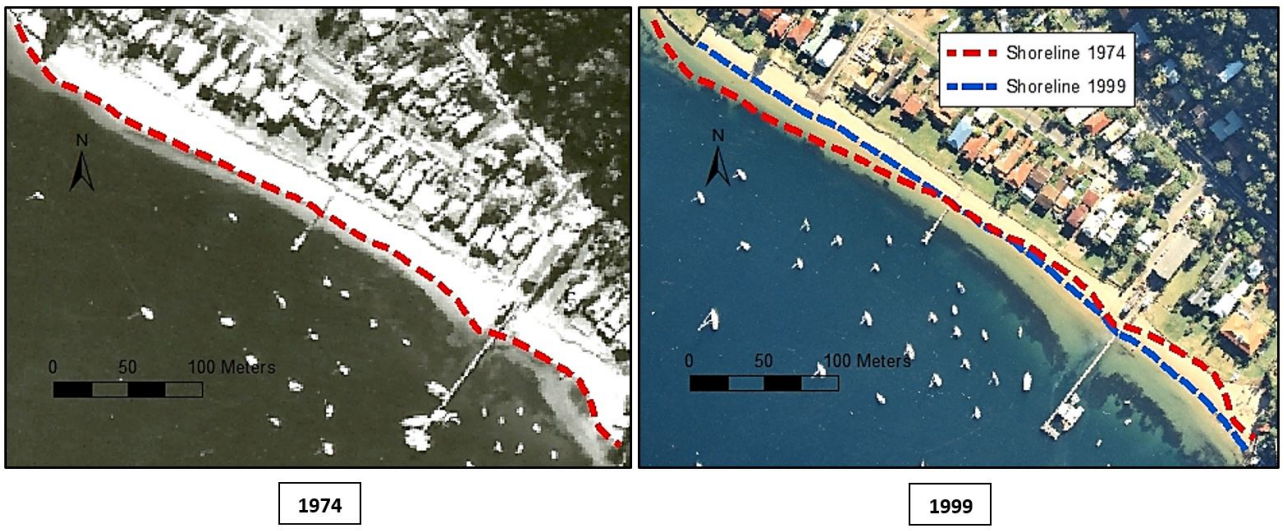

Figure 23: Clockwise rotation of Sandy Beach after the construction of the seawall in the northern part.

This phenomenon of accretion in the south of Sandy Beach is probably linked with the construction of a seawall in the early 1970s, on both sides of Sand Point (see Figure 24). According to Carley et al. (2010), altered erosion and accretion seaward from the wall or along the shore are potential physical impacts for this type of stabilization infrastructure. One hypothesis is that after the construction of the seawall, the sand located in front of it has been transported offshore. According to Cowell (1992), the transport of sand in the Pittwater estuary is preferably from north to south. Therefore, it is likely that the eroded sand has been transported alongshore and redeposited further south.

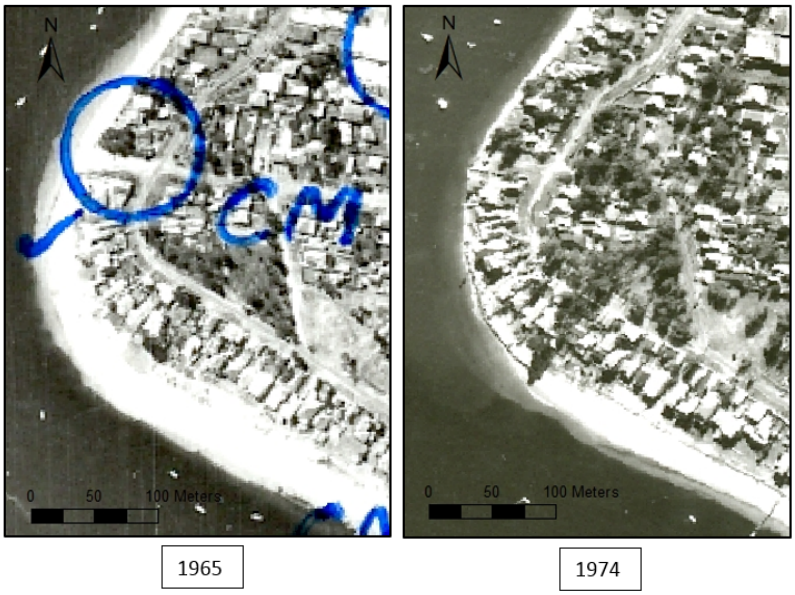

Figure 24: Construction of the seawall along Sand Point in the late 1960s. Possible cause of the disappearance of the beach between Snapperman and Sandy beach.

Great Mackerel Beach

For this beach, instead of using the profile n°5 to characterize the northern part of the beach, the profile n°4 was used (Figure 21 showing profile locations). This was done because the profile n°4 is located further away from the intertidal sand shoals at the northern end of the beach. Indeed, at the location of the profile n°5, the slope is lower and the shoreline is strongly affected by tidal variation (see cross-shore profiles on Figure 32).

Two distinct erosion and accretion periods can be observed on Figure 22d. First, until the late 1960s, the shoreline is moving seaward, expressing an accumulation of sediment in the upper foreshore of the beach. According to Thom (1974) during the period between the 1950s and late 1960s, there were no storm causing major beach erosion and it is reported as a period of beach accretion and foredune development in the Sydney region. Then, since the late 1960s, the photographs analysis indicate a landward displacement of the shoreline of approximately 30 m at the southern and northern extremity of the beach. The middle part of the beach was more stable with a landward displacement of around 15 m. In short, among the four study beaches, it is at Great Mackerel beach that the erosion was the greatest during the investigation period with a total recession of around 20 m at both extremity (see Table 7).

To explain the important shoreline recession observed at Great Mackerel, several factors have been identified. First, unlike the three other studied beaches, this one is located in the western part of the estuary and is more sensible to offshore generated waves arriving in the estuary (see Section 3.4.1). Another important factor is the presence of the stream mouth in the northern part of the beach that strongly influence the morphology of this beach. According to Cowell (1989), the strong erosion observed north from the wharf is mainly linked with the presence of this channel. Indeed, during erosion phase, sand is transported offshore and deposited in the basin formed by the channel. Therefore, because of this "delta-margin" process, sand is permanently lost from the natural onshore-offshore exchange cycle of the beach.

On Figure 22d, it is visible that the erosion caused by the storms of 1974 was important. According to Cowell (1992), this was a critical erosion period that put the northern-most beach-front properties in danger and it was mainly caused by the presence of the stream. Indeed, before 1974, a narrow partially-vegetated sand-barrier on the delta shoulder was deflecting the stream entrance against the northern headland and reducing the "delta-margin" effect. As shown on Figure 25, during the storm of 1974, this sand barrier has been destroyed and the stream mouth moved further to the south, aggravating the delta-margin erosion. On Figure 25, it is visible that this storm caused an important landward displacement of the vegetation line. With the presence of houses about ten meters from the dune line in the northern part of the beach, this erosion event had a strong effect on the local community that asked for protective measures and studies (Cowell, 1989, 1992). One protective measure was the reconstruction of the dune at the northern extremity of the beach and its stabilization with trees. This is visible on the aerial photo of 1996 on the Figure 25.

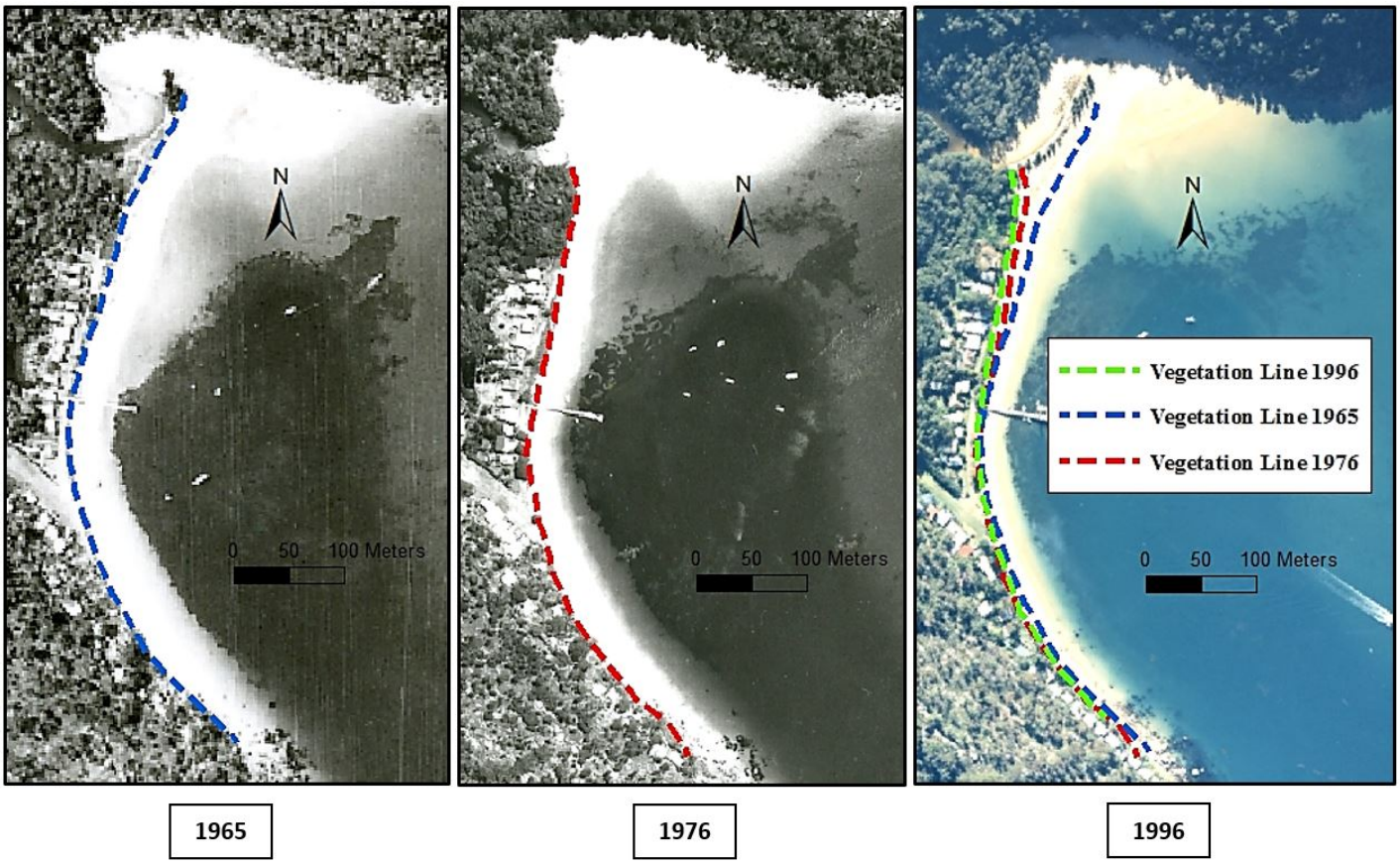

Figure 25: Aerial photographs of Great Mackerel beach showing the destruction of the sand barrier after the storm of 1974 and its reconstruction several years later. The dashed lines represent the position of the back of the beach, its evolution reflects the important erosion in the northern part of the beach after the storm of 1974.

Since the stream at the northern part of the beach drains a large catchment, its presence is also linked with some flood events at Great Mackerel beach that can cause strong erosion. In late 1988 - early 1989, a major flood happened causing a temporary discharge of the stream at the location of the northern-most houses (Cowell, 1989). As visible on the Figure 22d, the width of beach has been strongly reduced after this event.

Another factor that could explain the offshore losses of sand in Great Mackerel Beach is the seagrass decline in the Pittwater estuary between 1940 and 1960 (Kulmar et al., 1987). Indeed, the presence of seagrass beds on the lower shoreface has a sand-trapping effect that increase the shoreline stability. This reduction of seagrass coverage could be linked to the northwestern expansion of Sydney that has resulted in an increase of the level of pollution in the Hawkesbury river (Cowell, 1989).

5.2 Monthly to seasonally changes

5.2.1 Beach morphology

Following the criteria proposed by Short (1979), with an average slope of around 0.1 (tan β) and a width comprise between 10 and 20 m, the four studied beaches can be classified as sandy reflective beaches. This type of beach is generally steep and narrow with coarser sand and with average wave height less than 0.5 m on the NSW coast.

The beach morphology of the four studied sites have been monitored since May 2016. Below, a detailed analysis of these changes is conducted for each beach as well as between the different sections. To note that during this period of time, according to the Table 2, June 2016 and August 2017 appears to be the periods with greatest wave power.

Station Beach

Following the classification for sheltered beaches proposed by Hegge et al. (1996), Station Beach can be classified in the moderately steep group (see Section 2.3 for details about this classification). This type of beach is characterized by steep linear nearshore zones, wide beach face and high berms.

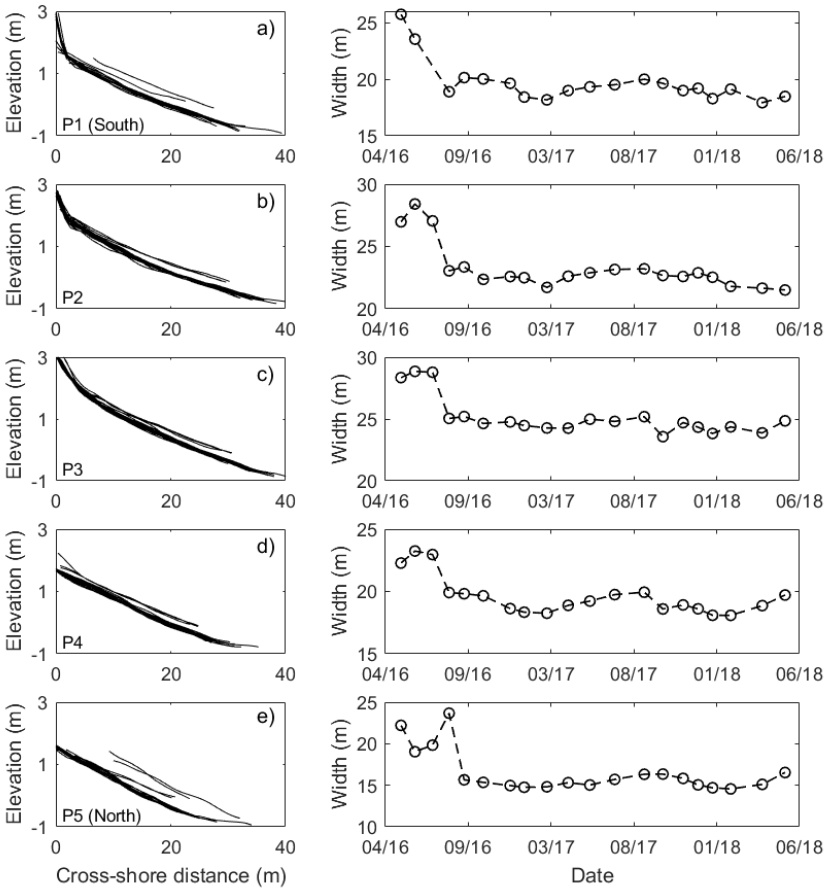

Figure 26: Station Beach cross-shore profiles surveys (May 2016 - May 2018). Left panels show the beach profiles and right panels the corresponding time series of beach width at the 0 m AHD contour elevation

After the storm of June 2016 which was an important erosion event, the five profiles behaved similarly to each other during the survey period and remained relatively stable in time. The June 2016

storm reduced the width of the beach by 3 to 5 m for profiles 1 to 4 and by almost 10 m for profile 5. A small diminution of the beach width can be observed after the storm of August 2017.

Snapperman Beach

With a steep and linear beachface slope, this beach can be classified as a steep beach according to Hegge et al. (1996). According to the profile change model of Nordstrom (1992), the parallel recession of beach profiles that can be observed on figure 27 is indicating that the dominant mode of sediment transport is long-shore rather than cross-shore.

The northern part of the beach (P1, P2 and P3) was the most dynamic part during the survey period with important width variations. The southern part (P4, P5 and P6) remained relatively stable.

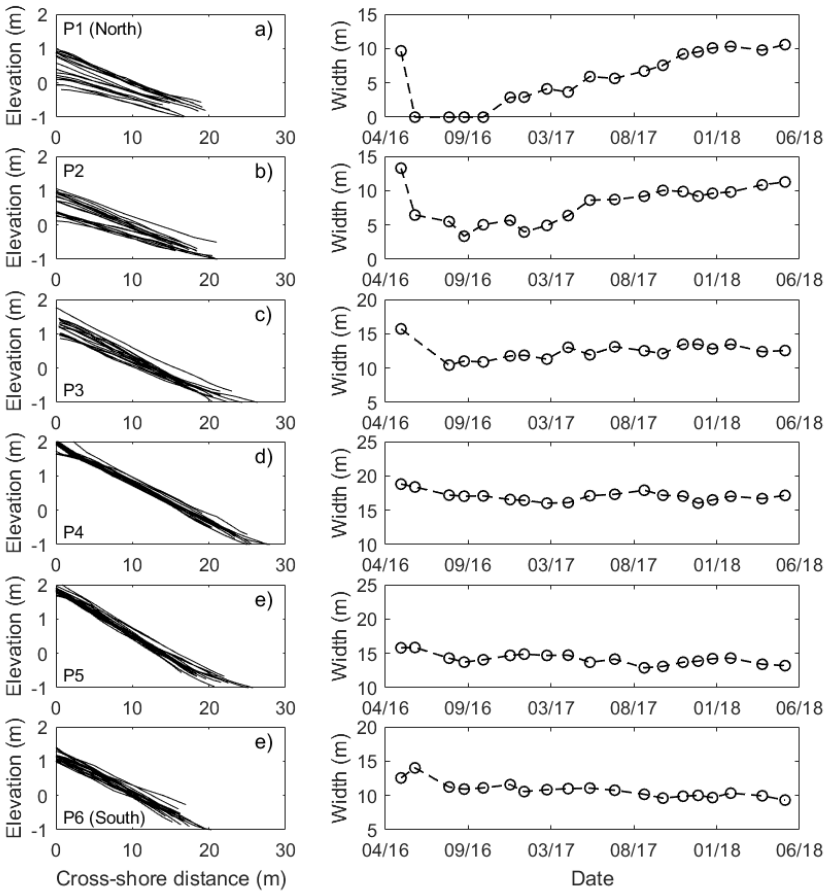

Figure 27: Snapperman Beach cross-shore profiles surveys (May 2016 - May 2018). Left panels show the beach profiles and right panels the corresponding time series of beach width at the 0 m AHD contour elevation

Sandy Beach

The northern part of the beach (profile 1, 2 and 3) is relatively steeper than the southern part of the beach (profile 4 and 5) that is characterized by a wider beach face. According to Hegge et al. (1996), the northern part of the beach can be classified as a steep beach while the southern part would probably belong to the moderately steep group. To note that the origin points of profiles 2 and 3 are located in the grass behind the dune, resulting in an abrupt change of slope at the landward part of these profiles.

Visible on the left panels of Figure 28, the shape of the profile 2 and 3 was modified during the monitoring period with an accretion of the upper foreshore part. According to the profile change model developed by Nordstrom (1992), deposition of sand in the upper-part of the foreshore indicate that the dominant mode of sediment transport is cross-shore rather than alongshore. For the other transects, no significant changes in the profile shape can be identified.

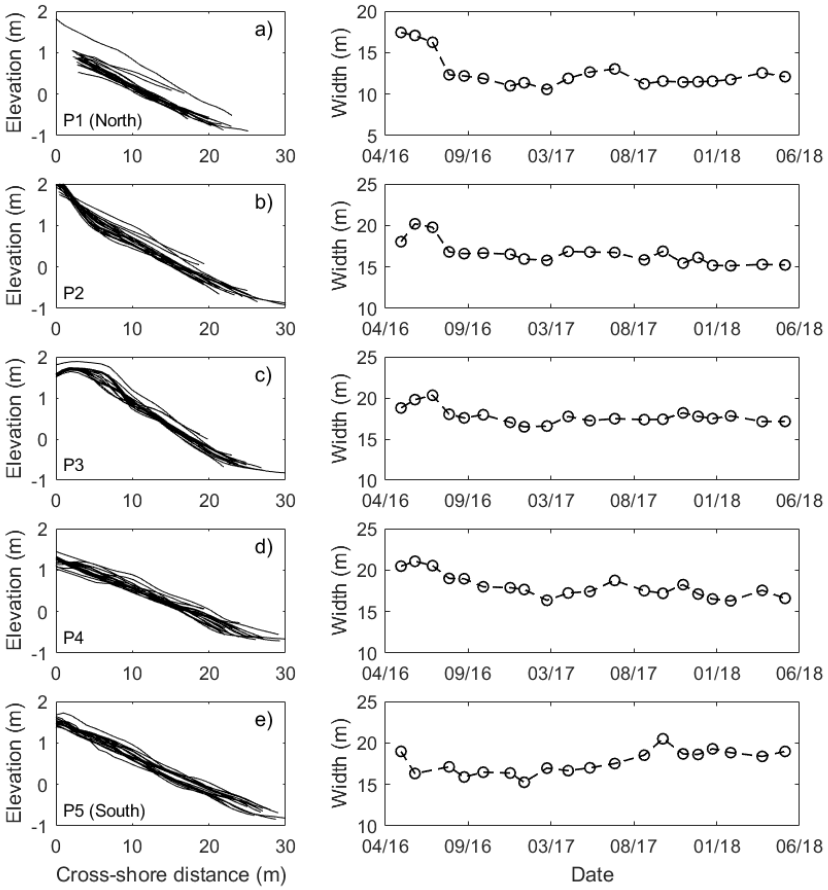

Figure 28: Sandy Beach cross-shore profiles surveys (May 2016 - May 2018). Left panels show the beach profiles and right panels the corresponding time series of beach width at the 0 m AHD contour elevation

Great Mackerel Beach

In terms of profile topographic shape, Great Mackerel appears to fall into two groups with the profiles 1, 2, 3 and 4 showing steep and linear beach face while the profile 5 is showing a more concave profile with a flatter nearshore zone. According to Hegge et al. (1996), sediment characteristics and groundwater conditions play an important part in the development of profile morphology. The presence of the stream mouth in the northern part of the beach could be the reason for the profile shape of transect 5. To note, the origin points of the profiles 2, 3 and 4 are located a few meters behind the dune crest, explaining why the upper extremity of these profiles didn't change in time.

By looking at the left panels on Figure 32, the northern part of the beach appears to be more dynamic than the southern part. According to the profile change model of Nordstrom (1992), the dominant sediment transport mode seems to be cross-shore with visible slope modification of the profiles 3, 4 and 5. These changes in profile shape are indicating that sand has been eroded at the upper part of the beach face and transported to the lower part.

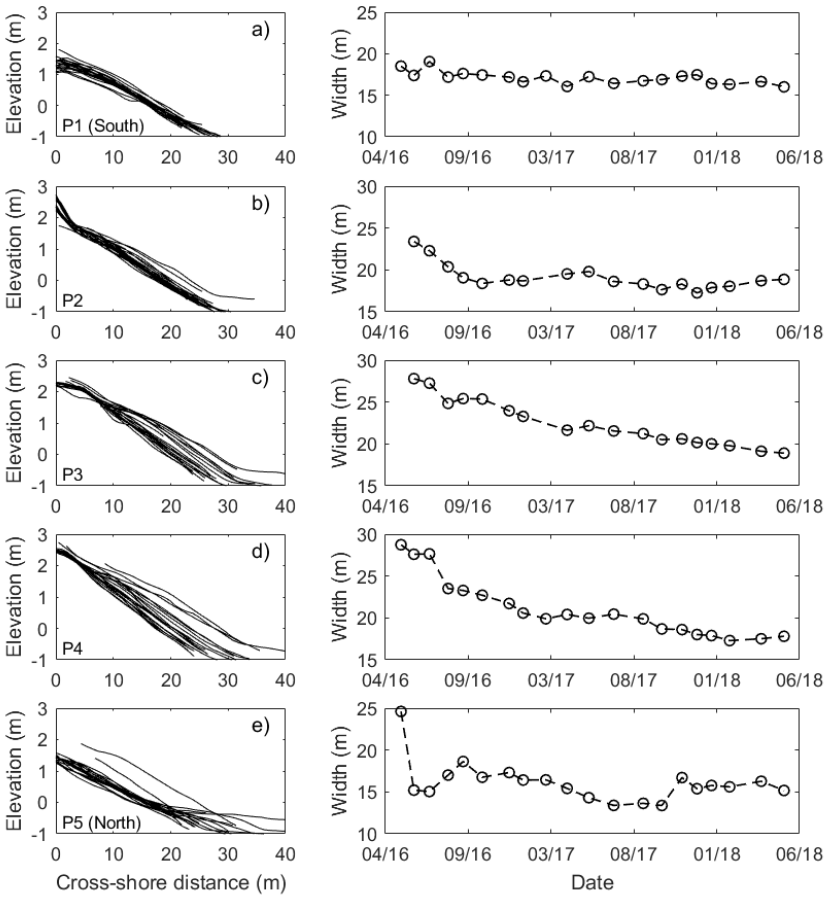

Figure 29: Great Mackerel Beach cross-shore profiles surveys (May 2016 - May 2018). Left panels show the beach profiles and right panels the corresponding time series of beach width at the 0 m AHD contour elevation

5.2.2 Erosion and post-storm recovery

The following chapters look at the subaerial beach volume changes that occurred between May 2016 and May 2018 for the different study sites. The subaerial volume changes as well as the percentage of volume recovery after the storm of June 2016 were calculated using the method presented in Section 4.2.2. The Figure 30 presents the results and is visible on the following page.

5.2.2.1 The Pittwater Estuary

Station Beach

As visible on the Figure 30(a), the profiles 1, 2, 3 and 4 were heavily affected by the June 2016 storms with a loss of volume of respectively 32%, 21%, 13% and 19% between the months of May and August 2016. The average subaerial volume change for Station beach was 4.08 $[m^3/m]$. According to the profile surveys (Figure 26), the part that was the more affected by the erosion was the lower foreshore part. A relevant point to note is that even though the high-energy event happened in June 2016, the consequences of the storm are visible on the profiles only in August, three months later.

Concerning the recovery of the beach, as it can be seen on Figure 30(a), the subaerial volume of the beach remained stable after this period and the beach has not yet recovered from this high-energy event.

Snapperman Beach

The June 2016 storms eroded a significant quantity of sand from the beach, especially in the northern part of the beach. Between the 20th May and the 16th June, the volume of profiles 1, 2 and 3 got reduced by 100%, 84% and 60% respectively. The southern part, profiles 4, 5 and 6 get less affected by the storm with around 20-25% of the initial volume being eroded. The mean subaerial change for the whole beach was 4.08 $[m^3/m]$ with a maximum value of 7.4 $[m^3/m]$ observed along profile 3. Concerning the storm of August 2017, the Figure 30(a) shows that the subaerial volume of the southern part of the beach got reduced by around 2 m.

Concerning the recovery, among the four studied sites, Snapperman beach is the one that has the best recovery rate after June 2016 storms. Figure 31(a) shows that after two years the beach has almost completely recovered along the profile 1 while around half of the volume have been recovered for profiles 2 and 3. Although the subaerial volume change was not really significant for the southern part of the beach, this part hasn't recovered and was even more eroded along the profile 5 and 6 (negative percentage of volume recovery after the storm).

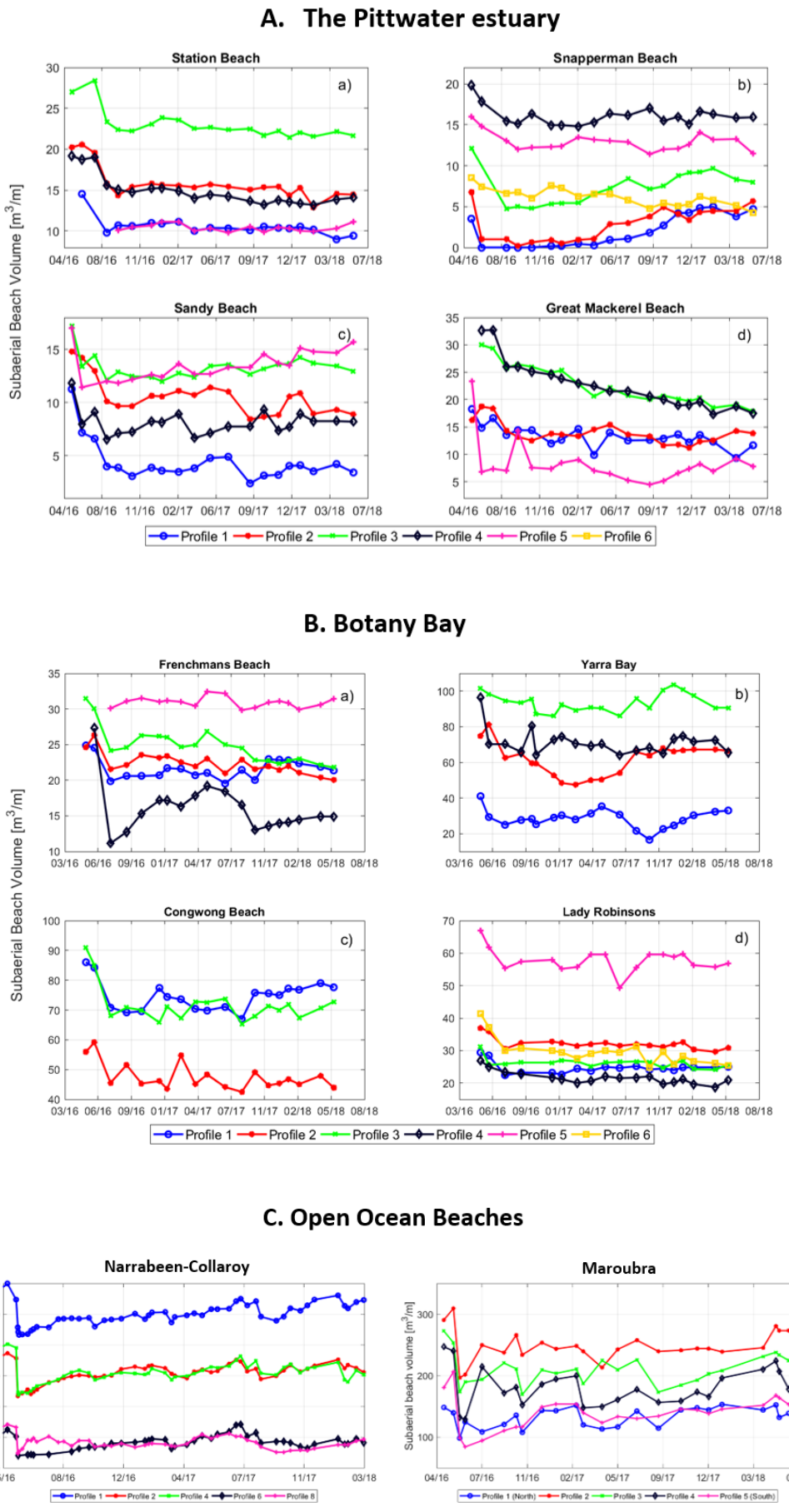

Figure 30: Volumetric changes of the subaerial part of the different study sites between May 2016 and June 2018

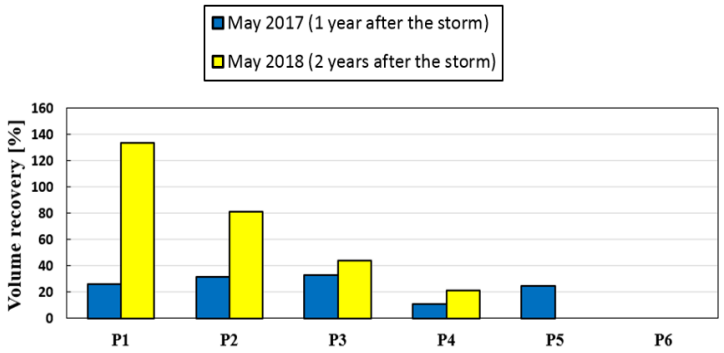

(a) Snapperman Beach

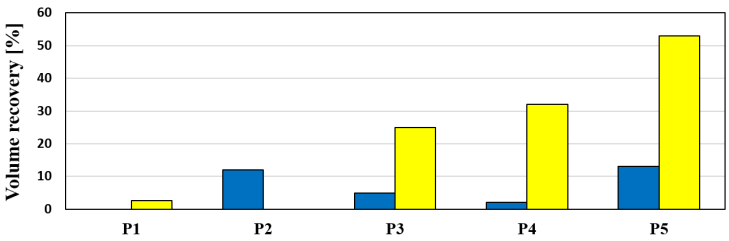

(b) Sandy Beach

Figure 31: Percentage of subaerial volume recovery, determined by reference to the subaerial volume lost after the storm of June 2016.

Sandy Beach

Between May 2016 and August 2016, significant changes of the subaerial volume of Sandy beach have been observed. Profile 1 was the most impacted with an erosion of 64% during this period of time while the others have seen their subaerial volume be reduced by around 30-40 %. For the whole beach, the mean subaerial change was 5.46 $[m^3/m]$ with a maximum value of 7.28 $[m^3/m]$ observed along profile 1. The part of the beach face that was the most eroded was the upper part of the foreshore (see Figure 27). Looking at the impact of the August 2017 storm, the northern part of Sandy Beach (profiles 1 and 2) has been affected by this event with a decrease of the subaerial volume of around 2 $[m^3/m]$.

Concerning the recovery after June 2016 storm, there is a strong contrast between the northern part of the beach and the southern part (Figure 31(b)). The northern part almost did not recover from the high-energy event and its volume continue to decrease in time. On the other hand, more than 50% of the volume eroded has been recovered at the southern part of the beach.

Great Mackerel Beach

Contrary to what was expected according to its exposition to ocean generated waves (see Section 3.4.1), Great Mackerel was affected in a similar way than the other studied beaches by the June 2016 storm. The volume reduction was between 10% and 25 % for the profiles 1, 2, 3 and 4. However, the northern part of the beach get strongly eroded with a subaerial volume change along the profile 5 of around 70%. For the whole beach, the mean subaerial change was 6.8 $[m^3/m]$ but the maximum value was 16.5 $[m^3/m]$ along profile 5.

Similar to Station Beach, Great mackerel shows no signs of recovery after the storm. Moreover, according to the subaerial volume evolution of the profile 3 and 4, the recession has continued in the northern part of the beach with a decrease in subaerial volume of 30 % and 32 % respectively

between August 2016 and May 2018. During the same period of time, the volume along the other profiles (1, 2 and 5) remained more stable.

Figure 32: The images on the left show the northern part of Snapperman beach (location of the profile n°2) and the images on the right show the middle part of Great Mackerel beach (location of the profile n°2). These photos were taken just before and after the storm of June 2016 as well as two years later.

5.2.2.2 Botany Bay

In order to compare the evolution of these two estuaries, the same method used to study short term changes in the Pittwater estuary has been applied to the data collected in Botany Bay. On Figure 30(b), it is visible that similar to the Pittwater estuary, Botany Bay was strongly affected by June 2016 storm. The consequences of the June 2016 storms vary from one beach to another. At Frenchmans Beach, the subaerial part of the profiles were eroded by around 20% for profiles 1, 2 and 3 and 60% for profile 4. The average subaerial volume change was 8 $[m^3/m]$. At Congwong Beach, the volume of the subaerial beach got reduced by around 20% with an average volume change of 16 $[m^3/m]$. The southern part of Lady Robinsons beach (profiles 5 and 6) have seen its subaerial volume reduced by around 40% while the rest of the beach (profiles 1, 2, 3 and 4) was eroded by around 20%. The average subaerial volume change was 7.5 $[m^3/m]$. Regarding Yarra Bay, it is harder to identify trends because this beach is highly variable in terms of beach volume.

Concerning the storm of August 2017, the erosion was less strong but some sections of Frenchmans, Yarra and Congwong beaches were significantly affected and this estuary was more affected by this storm than the Pittwater estuary (see Figure 30(b)). This difference is probably due to the orientation of the entrance. Indeed, the opening of Botany Bay is orientated in the south-east direction so more affected by waves coming from south to east sectors while the Pittwater estuary is more affected by waves coming from the east to north-east sectors.

The recovery of these beaches after the June 2016 storm is really low with only a few profiles that show signs of recovery. Among them, the profile 1 at Congwong beach recovered 45% of the eroded sand after 24 months. At Frenchmans Beach, the recovery along the profile 4 was great with 50% of volume recovery after 12 months but the storms of August 2017 again reduced the volume of sand to the same level as after the storm of June 2016. Concerning Lady Robinsons, the beach shows no sign of recovery two years after June 2016 storms and the volume of sand is similar to or lower than the level of August 2016 (except for profile 1 that has slightly recovered).

5.2.2.3 Narrabeen-Collaroy Beach

Subaerial beach volume have been obtained from the elevation data of Narrabeen-Collaroy that is freely available on http://narrabeen.wrl.unsw.edu.au/. The elevation data have been converted to subaerial beach volume volume using the methodology proposed by Harley et al. (2017b) and explained in Section 4.2.2.

According to Figure 30(c), Narrabeen-Collaroy beach was heavily impacted by June 2016 storms. The southern part of the beach (profile 6 and 8) was strongly eroded with around 60% of the subaerial beach volume eroded after June 2016 Storms. Profile 1, 2 and 4 have seen their volume reduced after the storm by 20, 32 and 38% respectively. The average total subaerial volume change was 109 $[m^3/m]$. The percentage of volume reduction is in the same order of magnitude with the ones observed in the Pittwater estuary and Botany Bay. Looking at the recovery after June 2016 storm, only three months after, the average percentage of subaerial beach recovery was 36%, 46% after six months and 49% one year later. To note that this beach was strongly affected by the storms of August 2017, more than the estuarine beaches of Botany Bay and the Pittwater estuary.

5.2.2.4 Maroubra Beach

As excepted according to its exposure, this beach was strongly eroded by the June 2016 storm, as visible on Figure 30(c). The volume of the northern part (profiles 1, 2 and 3) of the beach has been reduced by around 30% while the southern part (profiles 4 and 5) has seen his volume dropped by 45% and 51% respectively. The average subaerial volume change was 90 $[m^3/m]$. Similarly as for Narrabeen-Collaroy, the initial recovery of the beach was really fast with an average volume recovery equal to 39% after 3 months and 60% after 6 months. However, this good period of recovery was followed by some high-energy events and 2 years later the average volume recovery is still around 65%.

6 Discussion

In order to investigate the long term stability and the changes that occurred on a monthly to seasonal time scale, the present study has integrated two different time scales. Section 6.1 and 6.2 discuss the main shoreline changes observed in these two analysis and investigate the forcing mechanisms that lead to shoreline displacement. Section 6.3 look at the different rate of post-storm recovery between the study sites. The limitations of the present study and future research possibilities are presented in Section 6.4.

6.1 Decadal evolution

Long term shoreline analysis suggests that the beaches of the northern part of the Pittwater estuary have evolved differently during the period 1940-2017. Several factors could explain why the beaches have distinct long term trends. For example, it can be related to the influence of engineering interventions but also to the specific characteristics of the beach like the position in the estuary or the presence of a river outlet.

The beach that encountered the most long term recession since the 1940s is Great Mackerel Beach. As shown in the Section 5.1, two main erosive events were identified during the period of analysis, the storm of 1974 and the flood of 1989. In the Pittwater estuary, this beach is the most exposed from ocean generated waves and storm events are supposed to have greater impact on this beach than on the other studied beaches. In Section 5.1, it was shown that the 1974 storm changed the morphology of the northern part of Great Mackerel Beach by destroying a vegetated sand-barrier. The inability to recover after the 1974 storm supports the fact that low-energy beaches can be greatly impacted by storm waves that affect the long term shoreline evolution by changing the morphodynamic equilibrium of the system.

For the other studied beaches, according to the Figure 22, identification of the main erosive events with aerial images appears to be complicated because it is difficult to assess the effects of historic storms in the long term shoreline displacement results. On Figure 22, the only storm that induce distinctive beach width diminution is the storm of 1974 whose return period is 100 years. As mentioned by Smith and Zarillo (1990), to compare the effects of historic storms, aerial photos taken directly after the storms should be available. Especially if the time necessary for the beach to recover after a storm is shorter than the time interval between aerial photographs.

Beside from storms, stabilization infrastructure can also have important effects on the long term trends that have been observed by the aerial photographs. This hypothesis is supported by a recent study of the decadal evolution of the beaches in Botany Bay which is heavily urbanized (Schosberg, 2017). This study has reached the conclusion that the intensity of beach changes is correlated with the anthropogenic impacts on the hydrodynamics of the site. The Pittwater estuary is less impacted by stabilization infrastructures but the disappearance of the beach along Sand point and the accretion phenomenon occurring in the south part of Sandy Beach is probably linked with the construction of a seawall along Sand Point during the early 1970s. Moreover, this transport of sediment to the south of the beach is a concern for the Northern Beaches Council that asked for an investigation of the long term evolution of Sandy Beach (Manly Hydraulics Laboratory, 2012). The study concluded that the accretion of sand at the south of Sandy beach can put the use of certain infrastructures at risk, especially combined with the sea level rise. Constructions like the boat ramp will probably need some upgrades to maintain their serviceability in the future.

Figure 33: The northern part of Sandy Beach : an impressive dune scarp in the foreground and in the background, the seawall built around Sand Point.

Another factor to keep in mind when studying accretion and recession of beach is the supply of sediment. Indeed, since the inundation of estuaries along the southeast coast of Australia that occurred around 6.5 ka BP when global sea level rose, estuaries trap sediment coming from the land by the rivers or from the ocean by waves and tidal currents (Roy et al., 2001). The degree of infilling of estuaries is function of the sediment supply and accommodation space available. Roy et al. (2001) have developed a four class subdivisions to characterize the filling of estuaries, going from immature (Stage A, 0-25 % filled) to mature estuaries (Stage D, more than 75 % filled). In the same study, the Pittwater estuary has been classified as an unfilled estuary, filling up slowly since thousands of years. This result in a slowly growing marine flood tidal delta that is composed of sand from the open coast and influenced by tidal currents and wave action. However, the amount of marine sand available is finite and the sediment budget can be negative for certain estuarine beaches (Roy et al., 2001). In a study about the coastal processes of the Pittwater estuary (Kulmar et al., 1987), the authors indicate that the beaches along the western and eastern shore of the Pittwater estuary are the result of the longshore transport of sand from the marine delta located in the entrance of the estuary. The amount of sand is determined by the input of sand from the marine delta and the output of sand to the southern part of the estuary. In short, if the input of sand is lower than the level of the output, long term shoreline recession can occur. The variability of sand supply is also probably linked with the position of the beach in the estuary. Indeed, Palm Beach is located closer from the mouth of the estuary, the main sediment input source, and shows a relative stability in the long term analysis. On another hand, Great Mackerel and Snapperman beaches are located further away from the mouth of the estuary and show signs of long term recession.

6.2 Monthly to seasonal changes

Unlike the analysis of aerial photographs which aim to identify long term trends in shoreline displacement, topographic surveys allow to detect changes occurring over a short period of time, depending of the frequency of the surveys. A phenomenon that has been clearly identified with the

surveys data is the impact of June 2016 storm in the Pittwater estuary with an average diminution of the subaerial beach volume of 35% for the four studied beaches. These results confirmed that Pittwater is mostly exposed to ocean generated waves from northeast to east direction, like the June 2016 storm. Indeed, the storms of April and August 2017 with similar wave heights but from sector south had little impact in the Pittwater estuary, especially when compared with Botany Bay or other open ocean beaches like Maroubra or Narrabeen-Collaroy beach.

Another aspect that has been studied with survey results is the alongshore variability within a beach. With the exception of Station beach, for the three other studied sites, beach evolution was not similar between the different sectors. For example, at Snapperman beach, the northern part of the beach (profiles 1, 2 and 3) was strongly affected by June 2016 storm while the southern part (profiles 4, 5 and 6) remained more stable (see Figure 30(a)). One hypothesis to explain this strong alongshore variance could be the presence of hard stabilization infrastructures at the back of profiles 1 and 2 and at the northern extremity of Snapperman beach. During a storm, the presence of a seawall can intensify alongshore transport of material and inhibits beaches storm response (Pilkey and Wright III, 1988). The fast recovery observed at the northern part of Snapperman beach could also be linked with the seawall. Indeed, after the passage of the June 2016 storm, the morphology of the northern section of Snapperman beach was maybe far from its equilibrium state and therefore the return of sand to the upper foreshore was reinforced.

Figure 34: Illustration of the stabilization infrastructure in the northern part of Snapperman beach

During the last two years, alongshore variability was also observed at Sandy beach where accretion of sand occurred only at the southern part of the beach while the northern part was gradually eroded (visible on Figure 30(a)). As explained in the Section 5.1, this could be linked with the seawall around Sand Point that prevent sand deposition in the northern part of the beach and reinforced southward transport of material.

Concerning Great Mackerel beach, over the last two years, as visible in the Figure 30(a), the central part of the beach has decreased in volume while both extremity remained relatively stable. One explanation for the relative stability of profile 5 could be the presence of the sandy delta at the northern end of the beach which acts as a sand reservoir and allow this part of the beach to return more quickly to its equilibrium state. For the southern end, it is possible that this apparent stability is linked with southward transport of sand from the center and northern part of the beach. Indeed,

the zeta shape of the beach as well as its exposure from NE wind suggests southerly alongshore transport of sediment (Australian Water And Coastal Studies, 1991).

6.3 Post-storm recovery

In the Pittwater estuary and in Botany Bay, the process of post-storm recovery appears to be very slow and with great variance from one beach to another. In the first one, two beaches (Snapperman and Sandy beach) are showing some sign of recovery and in Botany Bay, recovery is observed only along few profiles. These results are in line with the statements of several authors (i.e. Costas et al. (2005), Jackson et al. (2002), Travers (2007), Vila-Concejo et al. (2010)). According to them, the morphology of estuarine beaches is inherited from high-energy events because the beaches do not have time to recover between these events. An extended period of fair weather conditions is necessary for a complete recovery of the beaches. As seen in Section 2.4, Jackson et al. (2002) identified two factors that could explain the slow recovery of estuarine beaches : restricted alongshore sediment supply and insufficient wave energy following a storm. However, by looking at the results of the long term shoreline analysis on Figure 22, except for Great Mackerel Beach and to a lesser extent Snapperman beach, no long term recession is observed. This can mean that estuarine beaches still recover the sand that is eroded during storms but at a really slow rate.

Observations of beach recovery in Narrabeen-Collaroy and Maroubra indicate a substantial recovery in only a relatively short amount of time. This show that, unlike estuarine beaches, exposed sandy beaches are naturally resilient to storms. According to Harley et al. (2017b), one important factor in post-storm recovery is exposition to the prevailing swell direction (southerly swell waves in NSW) that allow waves to bring back sand to the upper foreshore of the beaches. Another factor determining recovery rate is the waves conditions following a storm. The period of mild wave conditions prevailing after the June 2016 storm allowed a rapid recovery of the eroded sand.

6.4 Limitations and future research

The main limitation of the present study is the uncertainties related to the shoreline position extracted from aerial photographs, as seen in Section 4.1.4. This problem has been highlighted by several authors (i.e. Fletcher et al. (2003), Ruggiero et al. (2003), Smith and Zarillo (1990)). Indeed, uncertainty add "noise" to the results and only allow the identification of large long term trends that occur over several decades. Thus, the impacts of single event like storms or floods are difficult to identify in long term record. What can be done to reduce the total uncertainty is to correct the position of the shoreline according to the tidal level and the slope of the beach. Unfortunately, in the present study, it was not always specified at what time the photographs were taken and this correction was not possible to make for all the photographs.

Concerning the short term beach changes, forcing mechanisms and resulting beach changes were often based on previous studies or assumptions but not on real data. More field investigations would be necessary to have a better understanding of the physical processes that are taking place in the Pittwater estuary. A process that is poorly understood is the transport of sediment within the estuary. A time series of the bathymetry of the flood tidal delta could improve the knowledge about sand supply in the estuary. Also, the alongshore transport of sediment could be studied with measurement of nearshore currents for example. On another hand, the period covered by the topographic surveys doesn't allow to properly identify the time needed for estuarine beaches to recover from high-energy events and its crucial to continue the beach surveys in the future years.

7 Conclusion

By assessing the morphological changes of four beaches within the Pittwater estuary, at two different timescales, the present study is a contribution to the limited knowledge base of low-energy beach morphodynamics. Long term trends were derived by studying historical aerial photographs of the Pittwater estuary. Long term shoreline retreat was identified at Great Mackerel beach, the most exposed beach within the estuary. Concerning the three other beaches, they remained more stable over the last decades but shoreline rotation was observed at Sandy Beach, probably related to shoreline management interventions.

Data set obtained from the beach surveys campaign in the Pittwater estuary showed that storm events play the most important role in removing sediment from the beach, especially when the waves are coming from east to north-east direction. Also, strong alongshore variability were observed at three out of the four studied beaches within the Pittwater estuary. Concerning the beach recovery after severe storms, two years after the June 2016 storm, the percentage of volume recovery were very low in the Pittwater estuary as well as in Botany bay. The comparison with two open ocean beaches indicated that the post-storm recovery is much faster for these systems.

Most of the trends extrapolated from the historical photographs are supported by the beach surveys. Indeed, both analysis showed that Great Mackerel beach is experiencing strong erosion and that clockwise beach rotation is occurring at Sandy beach. Yet, when comparing the rate of change, they are much higher in the short term scale than in the long term one. Thus, while it is probably not a good idea to infer long term trends only with data sets that expand over a short period of time, this shows that long term trends could be observed with small scale data sets.

The findings of the present study could also be used to improve the future management of the beaches within the northern part of Pittwater estuary. This is especially relevant for the northern part of Great Mackerel Beach where the narrowing of this part of the beach could be a treat for some houses. Moreover, the accretion of sand in the southern part of Sandy beach could also put the use of some infrastructures like the boat ramp at risk.

8 Appendix

Appendix 1 : Detailed information about the images used for the long term analysis

Mackerel : Images used

Date	Area	Number of control points	RMS	Scale	Ground Resolution
		Aerial Images			
1941	Mackerel	6	1.80 [m]	-	-
01/01/1947	Mackerel	9	4.87 [m]	-	-
28/09/1955	All	10	1.74 [m]	-	-
23/09/1965	Mackerel	8	1.59 [m]	-	-
16/11/1976	All	13	1.39 [m]	1:16'000	-
01/04/1985	All	18	2.92 [m]	1:16'000	-
04/05/1990	Mackerel	7	0.64 [m]	1:8'000	-
19/04/1993	Mackerel	9	0.55 [m]	1:8'000	-
30/05/1996	Mackerel	9	1.09 [m]	1:8'000	-
22/04/2006	Mackerel	7	0.55 [m]	1:8'000	-
03/07/2008	Mackerel	9	0.62 [m]	1:8'000	-
		DigitalGlobe Images			
28/05/2005	All	-	-	-	1.2 [m]
		NearMap Images			
05/01/2013	All	-	-	-	0.6 [m]
23/02/2017	All	-	-	-	0.6 [m]

Table 8: Images used for the photogrammetric analysis of Great Mackerel Beach

Sandy Beach : Images used

Date	Area	Number of Control Points	RMS	Scale	Ground Resolution
		Aerial images			
29/09/1940	All	14	2.92 [m]	1:32'000	-
01/01/1947	All	9	1.38 [m]	-	-
01/05/1951	Snapperman-Sandy-Station	13	1.6 [m]	-	-
28/09/1955	All	10	1.74 [m]	-	-
23/09/1965	Snapperman-Sandy	11	2.76 [m]	-	-
19/06/1974	Snapperman-Sandy-Station	12	3.45 [m]	1:16'000	-
16/11/1976	All	13	1.39 [m]	1:16'000	-
01/04/1985	All	18	2.92 [m]	1:16'000	-
18/08/1990	Sandy	14	2.36 [m]	1:6'000	-
30/05/1996	Sandy	11	1.8 [m]	1:6'000	-
20/05/1999	Sandy-Snapperman	11	2.4 [m]	1:6'000	-
03/07/2008	Sandy-Snapperman	15	1.6 [m]	1:10'000	-
		DigitalGlobe Images			
28/05/2005	All	-	-	-	1.2 [m]
		NearMap Images			
05/01/2013	All	-	-	-	0.6 [m]
23/02/2017	All	-	-	-	0.6 [m]

Table 9: Images used for the photogrammetric analysis of Sandy Beach

Snapperman Beach : Images used

Date	Area	Number of Control Points	RMS	Scale	Ground Resolution
		Aerial images			
29/09/1940	All	14	2.92 [m]	1:32'000	-
01/01/1947	All	9	1.38 [m]	-	-
01/05/1951	Snapperman-Sandy-Station	13	1.6 [m]	-	-
28/09/1955	All	10	1.74 [m]	-	-
23/09/1965	Snapperman-Sandy	11	2.76 [m]	-	-
19/06/1974	Snapperman-Sandy-Station	12	3.45 [m]	1:16'000	-
16/11/1976	All	13	1.39 [m]	1:16'000	-
01/04/1985	All	18	2.92 [m]	1:16'000	-
18/08/1990	Snapperman	14	2.36 [m]	1:6'000	-
20/05/1999	Sandy-Snapperman	11	2.4 [m]	1:6'000	-
03/07/2008	Sandy-Snapperman	15	1.6 [m]	1:10'000	-
		DigitalGlobe Images			
28/05/2005	All	-	-	-	1.2 [m]
		NearMap Images			
05/01/2013	All	-	-	-	0.6 [m]
23/02/2017	All	-	-	-	0.6 [m]

Table 10: Images used for the photogrammetric analysis of Snapperman Beach

Station Beach : Images used

Date	Area	Number of Control Points	RMS	Scale	Ground Resolution
		Aerial images			
29/09/1940	All	14	2.92 [m]	1:32'000	-
01/01/1947	All	9	1.38 [m]	-	-
01/05/1951	Snapperman-Sandy-Station	13	1.6 [m]	-	-
28/09/1955	All	10	1.74 [m]	-	-
23/09/1965	Station Beach	11	2.76 [m]	-	-
19/06/1974	Station Beach	12	3.45 [m]	1:16'000	-
16/11/1976	All	13	1.39 [m]	1:16'000	-
28/03/1980	Station Beach	8	2.2 [m]	1:8'000	-
01/04/1985	All	18	2.92 [m]	1:16'000	-
18/08/1990	Station Beach	14	2.36 [m]	1:6'000	-
30/05/1996	Station Beach	11	1.29 [m]	1:6'000	-
20/05/1999	Station Beach	11	2.4 [m]	1:6'000	-
03/07/2008	Station Beach	15	1.6 [m]	1:10'000	-
		DigitalGlobe Images			
28/05/2005	All	-	-	-	1.2 [m]
		NearMap Images			
05/01/2013	All	-	-	-	0.6 [m]
23/02/2017	All	-	-	-	0.6 [m]

Table 11: Images used for the photogrammetric analysis of Station Beach

References

Austin, T., Short, A., Hughes, M., Vila-Concejo, A., and Ranasinghe, R. (2009). Tidal hydrodynamics of a micro-tidal, wave dominated flood-tide delta: Port stephens, australia. *Journal of Coastal Research*, pages 693–697.

Australian Water And Coastal Studies (1991). Design guidelines for water level and wave climate at pittwater. *Report prepared for Warringah Shire Council.*

Boak, E. H. and Turner, I. L. (2005). Shoreline definition and detection: a review. *Journal of coastal research*, pages 688–703.

Bryant, E. A. and Kidd, R. (1975). Beach erosion, may-june, 1974, central and south coast, nsw.

Callaghan, J. and Helman, P. (2008). Severe storms on the east coast of australia 1770–2008. *Griffith Centre for Coastal Management, Griffith University, Southport, Australia.*

Carley, J., Shand, T., Mariani, A., Shand, R., and Cox, R. (2010). Technical advice to support guidelines for assessing and managing the impacts of long term coastal protection works.

Costas, S., Alejo, I., Vila-Concejo, A., and Nombela, M. A. (2005). Persistence of storm-induced morphology on a modal low-energy beach: a case study from nw-iberian peninsula. *Marine Geology*, 224(1-4):43–56.

Cowell, P. J. (1989). Advisory report on management of beach erosion at Mackerel Beach. Technical report.

Cowell, P. J. (1992). *Mackerel Beach: Estimates of dune recession & nourishment demands due to raised sea levels & sand-budget variations.* . Coastal Studies Unit, University of Sydney.

Crowell, M., Leatherman, S. P., and Buckley, M. K. (1991). Historical shoreline change: error analysis and mapping accuracy. *Journal of coastal research*, pages 839–852.

Davies, J. (1964). 1964: A morphogenetic approach to world shorelines. zeitschrift fur geomorphologie 8, 127-44.

Eliot, M., Travers, A., and Eliot, I. (2006). Morphology of a low-energy beach, como beach, western australia. *Journal of Coastal Research*, pages 63–77.

Elliott, M. and McLusky, D. S. (2002). The need for definitions in understanding estuaries. *Estuarine, Coastal and Shelf Science*, 55(6):815–827.

Emery, K. (1961). A simple method of measuring beach profiles. *Limnology and oceanography*, 6(1):90–93.

Fairbridge, R. (1980). The estuary: its definition and chemical role. *Chemistry and Biochemistry of Estuaries. John Wiley and Sons, Chichester*, pages 1–35.

Fletcher, C., Rooney, J., Barbee, M., Lim, S.-C., and Richmond, B. (2003). Mapping shoreline change using digital orthophotogrammetry on maui, hawaii. *Journal of Coastal Research*, pages 106–124.

Haines, P., Fletcher, M., Rollason, V., and Coad, P. (2008). Lower hawkesbury estuary management plan. *BMT WBM Pty Ltd, Sydney.*

Hanslow, D. (2007). Beach erosion trend measurement: a comparison of trend indicators. *Journal of Coastal Research*, 50:588–593.

Harley, M. D., Turner, I. L., Kinsela, M. A., Middleton, J. H., Mumford, P. J., Splinter, K. D., Phillips, M. S., Simmons, J. A., Hanslow, D. J., and Short, A. D. (2017a). Extreme coastal erosion enhanced by anomalous extratropical storm wave direction. *Scientific reports*, 7(1):6033.

Harley, M. D., Turner, I. L., Middleton, J. H., Kinsela, M. A., Hanslow, D., Splinter, K. D., Mumford, P., et al. (2017b). Observations of beach recovery in se australia following the june 2016 east coast low. *Australasian Coasts & Ports 2017: Working with Nature*, page 559.

Harley, M. D., Turner, I. L., Short, A. D., and Ranasinghe, R. (2011). Assessment and integration of conventional, rtk-gps and image-derived beach survey methods for daily to decadal coastal monitoring. *Coastal Engineering*, 58(2):194–205.

Hegge, B., Eliot, I., and Hsu, J. (1996). Sheltered sandy beaches of southwestern australia. *Journal of Coastal Research*, pages 748–760.

Holland, G. J., Lynch, A. H., and Leslie, L. M. (1987). Australian east-coast cyclones. part i: Synoptic overview and case study. *Monthly Weather Review*, 115(12):3024–3036.

Houser, C., Wernette, P., Rentschlar, E., Jones, H., Hammond, B., and Trimble, S. (2015). Post-storm beach and dune recovery: Implications for barrier island resilience. *Geomorphology*, 234:54–63.

Jackson, N. L. (1995). Wind and waves: Influence of local and non-local waves on mesoscale beach behavior in estuarine environments. *Annals of the Association of American Geographers*, 85(1):21–37.

Jackson, N. L., Nordstrom, K. F., Eliot, I., and Masselink, G. (2002). 'low energy'sandy beaches in marine and estuarine environments: a review. *Geomorphology*, 48(1-3):147–162.

Kennish, M. J. (2016). *Encyclopedia of Estuaries (Encyclopedia of Earth Sciences Series).* Springer.

Kulmar, M., Gordon, A., et al. (1987). Coastal processes of the pittwater north western foreshores. In *Eighth Australasian Conference on Coastal and Ocean Engineering, 1987: Preprints of Papers*, page 109. Institution of Engineers, Australia.

Lord, D. and Kulmar, M. (2001). The 1974 storms revisited: 25 years experience in ocean wave measurement along the south-east australian coast. In *Coastal Engineering 2000*, pages 559–572.

Loureiro, C., Ferreira, Ó., and Cooper, J. A. G. (2012). Extreme erosion on high-energy embayed beaches: influence of megarips and storm grouping. *Geomorphology*, 139:155–171.

Makaske, B. and Augustinus, P. G. (1998). Morphologic changes of a micro-tidal, low wave energy beach face during a spring-neap tide cycle, rhone-delta, france. *Journal of Coastal Research*, pages 632–645.

Manly Hydraulics Laboratory (2015). 2015 Tide Charts. Technical report, NSW Public Works Manly Hydraulics Laboratory.

Manly Hydraulics Laboratory (April 2012). Sand point boat ramp, climate change impact assessment.

Maspataud, A., Ruz, M. H., and Héquette, A. (2009). Spatial variability in post-storm beach recovery along a macrotidal barred beach, southern north sea. *Journal of Coastal Research*, pages 88–92.

McBride, R. A., Hiland, M. W., Penland, S., Williams, S. J., Byrnes, M. R., Westphal, K. A., Jaffe, B. E., and Sallenger, A. H. (1991). Mapping barrier island changes in louisiana: techniques, accuracy, and results. In *Coastal Sediments*, pages 1011–1026. ASCE.

Mills, G. A., Webb, R., Davidson, N. E., Kepert, J., Seed, A., and Abbs, D. (2010). The pasha bulker east coast low of 8 june 2007. *Centre for Australia Weather and Climate Research Tech. Rep*, 23:62.

Mortlock, T. R., Goodwin, I. D., McAneney, J. K., and Roche, K. (2017). The june 2016 australian east coast low: Importance of wave direction for coastal erosion assessment. *Water*, 9(2):121.

Morton, R. A., Paine, J. G., and Gibeaut, J. C. (1994). Stages and durations of post-storm beach recovery, southeastern texas coast, usa. *Journal of Coastal Research*, pages 884–908.

Nordstrom, K. (1992). *Estuarine beaches*. Elsevier.

Nordstrom, K. F. and Jackson, N. L. (2012). Physical processes and landforms on beaches in short fetch environments in estuaries, small lakes and reservoirs: A review. *Earth-Science Reviews*, 111(1-2):232–247.

Novak, K. (1992). Rectification of digital imagery. *Photogrammetric engineering and remote sensing*, 58:339–339.

NSW Government (1992). Estuary management manual. Technical report.

Pilkey, O. H. and Wright III, H. L. (1988). Seawalls versus beaches. *Journal of Coastal Research*, pages 41–64.

Pittwater Council (2006). *Snapperman Beach Reserve - Palm Beach: Plan of management*. Warriewood, N.S.W. : Pittwater Council.

Pritchard, D. W. (1967). Observations of circulation in coastal plain estuaries. *Estuaries*.

Public Works Department, N.S.W (1982). Palm Beach - Beach Erosion and Management Study. Technical Report 82027.

Public Works Department, N.S.W (1986). Summary of storm damage and associated sea and weather conditions on the N.S.W coast - 1876 to 1981. Technical Report 86014.

Qin, D., Chen, Z., Averyt, K., Miller, H., Solomon, S., Manning, M., Marquis, M., and Tignor, M. (2007). Ipcc, 2007: Summary for policymakers.

Robert, S. (2004). Heritage Assessment, Palm Beach 2108, 22 Iluka road.

Rocchini, D., Metz, M., Frigeri, A., Delucchi, L., Marcantonio, M., and Neteler, M. (2012). Robust rectification of aerial photographs in an open source environment. *Computers & geosciences*, 39:145–151.

Roper, T., Creese, B., Scanes, P., Stephens, K., Williams, R., Dela-Cruz, J., Coade, G., Coates, B., and Fraser, M. (2011). Assessing the condition of estuaries and coastal lake ecosystems in nsw.

Roy, P., Williams, R., Jones, A., Yassini, I., Gibbs, P., Coates, B., West, R., Scanes, P., Hudson, J., and Nichol, S. (2001). Structure and function of south-east australian estuaries. *Estuarine, Coastal and Shelf Science*, 53(3):351–384.

Ruggiero, P., Kaminsky, G. M., and Gelfenbaum, G. (2003). Linking proxy-based and datum-based shorelines on a high-energy coastline: implications for shoreline change analyses. *Journal of Coastal Research*, pages 57–82.

Schosberg, R. (2017). *Monthly to decadal morphologic evolution of sheltered beaches within an urbanized estuary*. PhD thesis, University of Sydney.

Shand, T., Goodwin, I., Mole, M., Carley, J., Browning, S., Coghlan, I., Harley, W., You, Z., and Kulmar, M. (2010). Nsw coastal storms and extreme waves. In *19th Annual Coastal Conference Coffs Harbour*.

Short, A. (1979). Three dimensional beach-stage model. *The Journal of Geology*, 87(5):553–571.

Short, A. D. (2007). *Beaches of the New South Wales coast: a guide to their nature, characteristics, surf and safety*. Sydney University Press.

Short, A. D. and Trembanis, A. C. (2004). Decadal scale patterns in beach oscillation and rotation narrabeen beach, australia—time series, pca and wavelet analysis. *Journal of Coastal Research*, pages 523–532.

Short, A. D. and Trenaman, N. (1992). Wave climate of the sydney region, an energetic and highly variable ocean wave regime. *Marine and Freshwater Research*, 43(4):765–791.

Shoshany, M. and Degani, A. (1992). Shoreline detection by digital image processing of aerial photography. *Journal of Coastal Research*, pages 29–34.

Smith, G. L. and Zarillo, G. A. (1990). Calculating long-term shoreline recession rates using aerial photographic and beach profiling techniques. *Journal of Coastal Research*, pages 111–120.

Thom, B. and Hall, W. (1991). Behaviour of beach profiles during accretion and erosion dominated periods. *Earth Surface Processes and Landforms*, 16(2):113–127.

Thom, B. G. (1974). Coastal erosion in eastern australia. *Search, Sci Technol Soc*.

Travers, A. (2007). Low-energy beach morphology with respect to physical setting: a case study from cockburn sound, southwestern australia. *Journal of Coastal Research*, pages 429–444.

Turner, I. L., Harley, M. D., Short, A. D., Simmons, J. A., Bracs, M. A., Phillips, M. S., and Splinter, K. D. (2016). A multi-decade dataset of monthly beach profile surveys and inshore wave forcing at narrabeen, australia. *Scientific data*, 3:160024.

Vila-Concejo, A., Hughes, M. G., Short, A. D., and Ranasinghe, R. (2010). Estuarine shoreline processes in a dynamic low-energy system. *Ocean Dynamics*, 60(2):285–298.

Watson, P. and Lord, D. (2008). Fort denison sea level rise vulnerability study. *Report prepared by the Coastal Unit, NSW Department of Environment and Climate Change*.